FERMILAB-PUB-91/180-A

Limits to the radiative decay of the axion

M. Ted Ressell
Department of Astronomy and Astrophysics, Enrico Fermi Institute, The University of Chicago, Chicago, Illinois 60637-1433
and NASA/Fermilab Astrophysics Center, Fermi National Accelerator Laboratory, Batavia, Illinois 60510-0500
(Received 28 June 1991)

An axion with a mass greater than 1 eV should be detectable through its decay into two photons. In this paper I discuss the astrophysical and cosmological limits which define a small window of allowed axion mass above 3 eV. A firm upper bound to the axion's mass of $m_a \leq 8$ eV is derived by considering the effect of decaying axions upon the diffuse extragalactic background radiation and the brightness of the night sky due to axions in the halo of our Galaxy. The intergalactic light of clusters of galaxies is shown to be an ideal place to search for an emission line arising from the radiative decay of axions. An unsuccessful search for this emission line in three clusters of galaxies is then detailed. Limits to the presence of any intracluster line emission are derived with the result that axions with masses between 3 and 8 eV are excluded by the data, effectively closing this window of axion mass, unless a severe cancellation of axionic decay amplitudes occurs. The intracluster flux limits are then used to constrain the amplitude of any such model dependence.

I. INTRODUCTION

Astrophysical and cosmological considerations have led to numerous constraints on new particle-physics phenomena. Nowhere has the interplay of these disciplines been more apparent than in the search for the axion [1,2]. The axion is a direct consequence of a modest and desirable extension of the standard model of particle physics, Peccei-Quinn (PQ) symmetry [3]. PQ symmetry was originally proposed as a solution to the strong *CP* problem of quantum chromodynamics (QCD). PQ symmetry also arises naturally in theories of supersymmetry and superstrings.

As a result of the nontrivial topology of the QCD vacuum, the strong interactions violate *CP* invariance with a strength proportional to a parameter Θ. This *CP* violation manifests itself in a number of ways, most notably in the electric dipole moment of the neutron, d_n. QCD predicts a value of roughly $d_n \simeq 5\times10^{-16}\,\bar{\Theta}\ e$ cm, while the experimentally determined value is $d_n \lesssim 10^{-25}\ e$ cm and $\bar{\Theta}=\Theta+\mathrm{Arg\,det}\mathcal{M}$, where $\mathcal{M}$ is the quark mass matrix. This leads to the constraint $\bar{\Theta}\lesssim 10^{-9}$–$10^{-10}$. A value of $\bar{\Theta}$ this small violates the naive expectation that a dimensionless parameter of a theory should have a value of order 1 and is unnatural in the sense defined by 't Hooft [4,5]. The strong *CP* problem is, in essence, the question why is $\bar{\Theta}$ so small?

The PQ solution solves this problem by introducing a new global U(1) symmetry into the theory. This $U(1)_{PQ}$ is then spontaneously broken at an energy scale f_{PQ}, where I follow the notation of Ref. [1]. The pseudo Nambu-Goldstone boson associated with this symmetry breaking is the axion [6]. $U(1)_{PQ}$ is not an exact symmetry; it is broken by QCD anomalies at the quantum level. Because of this explicit breaking the axion acquires a small mass which is inversely proportional to the scale of spontaneous symmetry breaking:

$$m_a = \frac{\sqrt{z}}{1+z}\frac{f_\pi m_\pi}{f_{PQ}/N} \simeq \frac{0.62\ \mathrm{eV}\times10^7\ \mathrm{GeV}}{f_{PQ}/N}\ , \tag{1}$$

where N is the color anomaly of the PQ symmetry, $z=m_u/m_d\simeq0.56$, $f_\pi=93$ MeV, and $m_\pi=135$ MeV. (Throughout I refer to the axion's mass in terms of its rest energy $m_a c^2$.) In addition, the axion's couplings to matter are inversely proportional to f_{PQ} (or equivalently, proportional to m_a). At the time of the QCD confinement phase transition the axion potential develops a minimum which corresponds to $\bar{\Theta}=0$. As the axion relaxes to the minimum of its potential it forces $\bar{\Theta}=0$, thus solving the strong *CP* problem.

There are two generic types of axions. Dine-Fischler-Srednicki-Zhitnitskii (DFSZ) axions couple to both quarks and leptons at tree level [7]. The hadronic, or Kim-Shifman-Vainshtein-Zakharov (KSVZ), axion has no tree-level couplings to leptons but does couple to them through loop diagrams [8]. Throughout the remainder of this paper I will focus on the hadronic axion, as DFSZ axions more massive than 1 eV have been ruled out by stellar-evolution arguments [1,2]. Since DFSZ axions couple directly to electrons, they can be profusely emitted from the cores of stars. This provides a very efficient means of transporting energy from the core to interstellar space. For masses greater than 1 eV a DFSZ axion would so strongly effect the core of the Sun that its existence could not have gone unnoticed. This lower bound to m_a (DFSZ) is further strengthened by considering the effect of axions upon red-giant stars. These mass bounds on DFSZ axions escape much of the model dependence which is present in similar bounds to the hadronic axion (as discussed in the next section) and are much stronger since the direct *aee* coupling is much stronger than the equivalent coupling for the hadronic axion.

Axions can decay into two photons. The $a\gamma\gamma$ coupling arises due to two different decay mechanisms: through

axion-pion mixing and via the electromagnetic (EM) anomaly of PQ symmetry:

$$\mathcal{L}_{a\gamma\gamma}=-\frac{1}{4}\frac{\alpha/2\pi}{f_{\rm PQ}/N}\left[\frac{E}{N}-1.95\right]aF^{\mu\nu}\tilde{F}_{\mu\nu}$$
$$=\frac{a/2\pi}{f_{\rm PQ}/N}\left[\frac{E}{N}-1.95\right]a\mathbf{E}\cdot\mathbf{B}\ ,$$

where $\alpha\simeq\frac{1}{137}$, $F^{\mu\nu}$ is the EM field strength tensor and $\tilde{F}_{\mu\nu}$ is its dual, $1.95=2(4+z)/3(1+z)$, and E is the value of the EM anomaly of PQ symmetry. The axion decay width to two photons is

$$\Gamma_a=\tau_a^{-1}=\frac{1}{2^8\pi^3}\frac{\alpha^2}{(f_{\rm PQ}/N)^2}\left[\frac{E}{N}-1.95\right]^2 m_a^3\ ,$$

which leads to an axion lifetime of

$$\tau_a(a\to 2\gamma)\simeq 6.8\times 10^{24}\zeta^{-2}(m_a/\text{eV})^{-5}\,\text{sec}\ , \qquad (2)$$

where I have introduced the notation $\zeta=|(E/N-1.95)|/0.72$. In the simplest models which incorporate axions, $E/N=\frac{8}{3}$ and $\zeta=1$. While $E/N=\frac{8}{3}$ is the value that arises when the axion is incorporated into the simplest unified models it is not required; models with, for example, $E/N=2$ are easily constructed [9]. For models of this type, $\zeta=0.07$ and the two-photon decay of the axion is highly suppressed due to the near cancellation of the amplitudes from the EM anomaly and axion-pion mixing. (It should be noted that since the value 1.95 in the above formulas depends upon the uncertain ratio of the up- and down-quark masses, it too is not an exact value. In fact, within the allowed quark mass errors, a value of $\zeta=0$ for $E/N=2$ is possible, leading to a stable axion. Throughout the remainder of this paper I will regard $\zeta=0.07$ as a benchmark lower limit to the value of this parameter, but it should be kept in mind that its value could be smaller.) The parameter ζ is of great importance when considering astrophysical limits to the mass of the axion.

While the properties of the axion are well defined in terms of $f_{\rm PQ}$ (or m_a), this quantity has no preferred value. $f_{\rm PQ}$ might plausibly lie anywhere in the range 10^2 to 10^{19} GeV, corresponding to axion masses of 100 keV$\gtrsim m_a\gtrsim 10^{-12}$ eV. Astrophysical and cosmological arguments have been extremely useful in narrowing this allowed range. Because of many clever arguments there are but two "windows" of mass left open to the axion: $10^{-6}\lesssim m_a\lesssim 10^{-3}$ eV and, for the hadronic axion only, $3\lesssim m_a\lesssim 8$ eV. The latter window is the subject of this paper. In the next section I will review the arguments that define the boundaries of the multi-eV window; more complete reviews appear in Refs. [1] and [2].

Axions, if they exist in either of the windows of allowed mass, will have cosmologically interesting and potentially detectable relic abundances. The dominant production mechanisms in the two windows differ significantly. In the lower mass window, axions are produced through two different coherent mechanisms: misalignment production and axionic string decay. Both of these processes are highly nonthermal and both can produce nearly the critical density in axions if m_a lies in the mass range $10^{-3}\gtrsim m_a\gtrsim 10^{-6}$ eV. As an example, the misalignment mechanism typically produces axions with an abundance [10,11]

$$\Omega_a(\text{mis})h_{50}^2\simeq 3.4\times 10^{\pm 0.4}\times\left[\frac{\Lambda_{\rm QCD}}{200\ \text{MeV}}\right]^{-0.7}\left[\frac{m_a}{10^{-5}\ \text{eV}}\right]^{-1.18}\ , \qquad (3)$$

where $\Lambda_{\rm QCD}\simeq 150$–$400$ MeV is the QCD scale parameter. This abundance can be significantly altered, upwards or downwards, if inflation occurred after the PQ transition or axionic string decay is the dominant axion production mechanism (see Refs. [1,2,10,11] for complete details). As Eq. (3) demonstrates, an axion with a mass lying in the lower mass window will quite likely make up a sizable fraction of the dark matter in the Universe. Axions with masses above 10^{-2} eV are produced thermally. Since the coupling of the axion to normal matter is proportional to m_a, axions eventually couple strongly enough to thermalize. This happens for axions with masses greater than 10^{-2} eV [10,12]. Thus, axions in the multi-eV window are thermally produced and have an abundance similar to

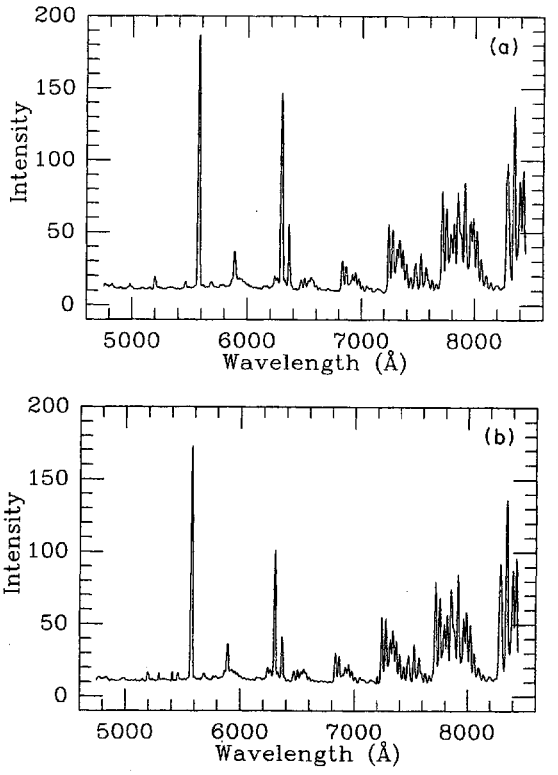

FIG. 1. Spectra of two intergalactic regions in the cluster A1413, night 1. (a) The inner, or "on," aperture ($R/a=1.11$); (b) the outer, or "off," aperture ($R/a=4.64$). Intensity is in units of 10^{-18} erg cm^{-2} arc sec^{-2} Å^{-1} sec^{-1}.

that of microwave background photons and relic neutrinos.

Once these axions are produced, where are they likely to be found? Since the current temperature of the microwave background radiation is $T_{\gamma 0} \simeq 2.4 \times 10^{-4}$ eV, axions are nonrelativistic and have been since before decoupling. Therefore axions should, in accord with the equivalence principle, fall with baryons and any other particles into the various potential wells which develop in the Universe. The most likely place to find relic axions with masses of a few eV is in clusters of galaxies and the halos of galaxies (as the axions have no way of dissipating their energy to condense further). As I will show later, phase-space considerations make clusters of galaxies the most likely hunting ground for these axions.

If these multi-eV axions reside in clusters of galaxies, as seems likely, their decay into two photons provides a powerful way of searching for them [12,13]. Decaying axions will produce an emission line at a wavelength $\lambda_a(z) \simeq 24\,800$ Å $(\mathrm{eV}/m_a)(1+z)$, where z is the cluster's redshift. This line will be Doppler broadened by the velocities axions have in the cluster to a width of $\Delta\lambda_a \sim 100$ Å and will have an intensity of $I_a \sim 1.5 \times 10^{-17} (m_a/3\ \mathrm{eV})^7 \zeta^2$ erg cm^{-2} arc sec^{-2} Å^{-1} sec^{-1}. In any attempt to detect this feature the signal must compete with the brightness of the night sky (NS). The night sky is characterized by a continuum intensity level of $I_{\mathrm{NS}} \sim 10^{-17}$ erg cm^{-2} arc sec^{-2} Å^{-1} sec^{-1} and many strong atmospheric emission lines [14] (see Figs. 1–5). In this paper I give a detailed account of an unsuccessful telescopic search for an axionic decay line in three clusters of galaxies. The search was conducted at Kitt Peak National Observatory (KPNO) and no axion decay line was detected, effectively closing the 3–8 eV window of axion mass.

I close the introductory comments by noting that while the search was motivated by the axion, our results are quite general. They can place meaningful constraints upon any relic particle species which decays to one or more photons and which clusters with galaxies, e.g., massive neutrinos [15]. Even more generally, the results place limits on the presence of any diffuse intergalactic line emission in clusters of galaxies, no matter what the source.

II. THE WINDOW

The 3–8 eV axion window is defined by a number of different arguments. The lower mass boundary is determined by the axion's effect upon SN 1987A and its observed neutrino burst [16]. The upper boundary is deter-

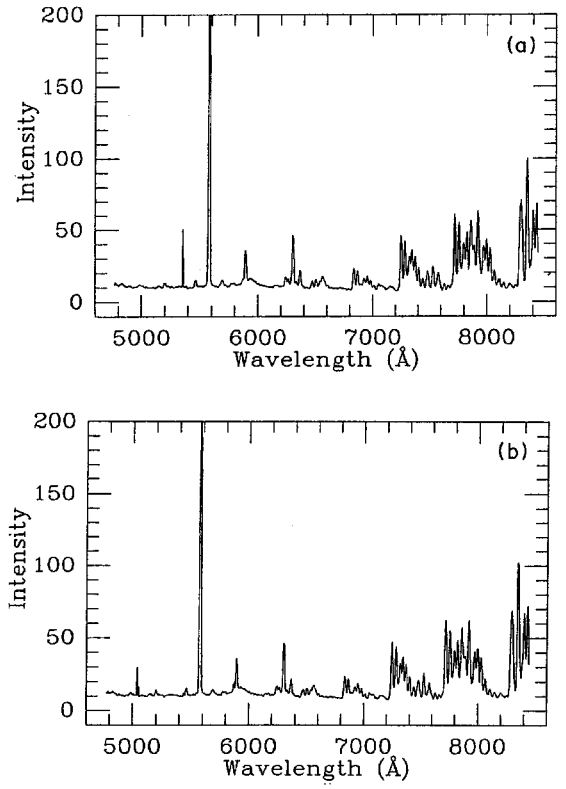

FIG. 2. Spectra of two intergalactic regions in the cluster A2218, night 1. (a) The inner, or "on," aperture ($R/a = 0.94$); (b) the outer, or "off," aperture ($R/a = 5.33$). Intensity is in units of 10^{-18} erg cm^{-2} arc sec^{-2} Å^{-1} sec^{-1}.

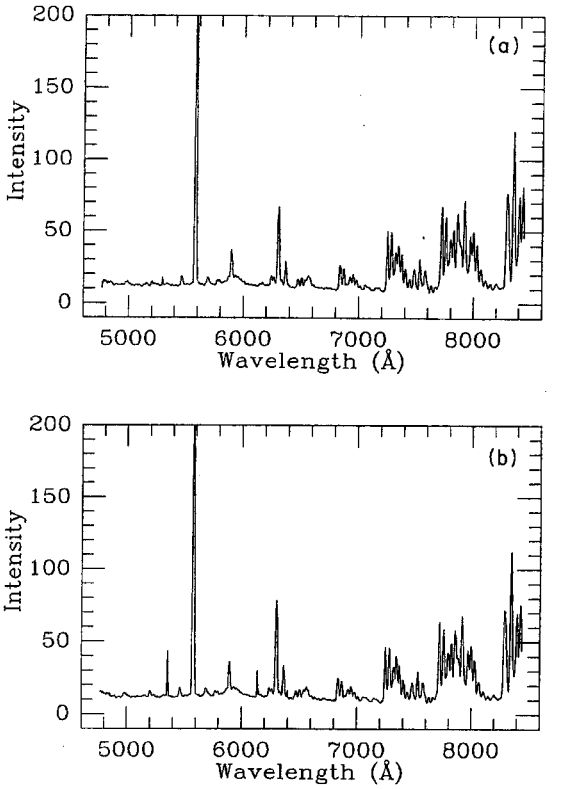

FIG. 3. Spectra of two intergalactic regions in the cluster A2256, night 1. (a) The inner, or "on," aperture ($R/a = 0.48$); (b) the outer, or "off," aperture ($R/a = 2.96$). Intensity is in units of 10^{-18} erg cm^{-2} arc sec^{-2} Å^{-1} sec^{-1}.

mined by several very different considerations. The first of these is the effect of axion emission upon the life cycle of red-giant (RG) and horizontal-branch (HB) (i.e., helium-burning) stars [17,18]. The second is the effect of SN 1987A emitted axions upon nuclei in the Kamiokande II (KII) detector [19]. The last is the effect of decaying axions upon the diffuse extragalactic background radiation (DEBRA) [12,20].

The effects of axions upon SN 1987A have been considered by numerous authors (see Refs. [1,2], and references therein) with the result that axions in the mass range $10^{-3} \lesssim m_a \lesssim 3$ eV are not compatible with the observations and therefore excluded. Here I will sketch the argument which leads to the upper bound of 3 eV (for details see Refs. [16,21]). As the axion's mass is increased, it couples more and more strongly to "normal" matter. At masses greater than about 10^{-3} eV the axion couples strongly enough so that it is profusely emitted by the core of a hot young neutron star during a supernova explosion, but not so strongly so that the matter seriously impedes the axion energy flux out of the star. This flow of energy out of the core severely depletes the reservoir of heat which powers the later phase of neutrino emission, severely shortening the neutrino burst. As the axion mass is increased beyond 10^{-3} eV the axion couples even more strongly, and at a mass of about 10^{-2} eV the axion's mean free path becomes less than the radius of the neutron star; axions are trapped, much like the neutrinos. This axion trapping reduces the flux of axion energy leaving the neutron star. As the axion mass is further increased the trapping becomes so strong that, like photons, the axions carry too little energy to seriously effect the neutrino burst.

The greatest observable effect of axions upon the supernova neutrino burst is in the burst duration. By incorporating axion emission into numerical models of protoneutron star formation, the authors of Ref. [16] determined that the SN 1987A neutrino burst observed in the KII and Irvine-Michigan-Brookhaven (IMB) detectors would be shortened by a factor of 2 or more for axions with masses less than 3 eV (and more than 10^{-3} eV). This constitutes the lower bound of the multi-eV window. There are a number of uncertainties in this limit. For example, the exclusion criterion of requiring the neutrino burst to decrease by a factor of 2, while reasonable, is rather arbitrary. Also, while the relevant axion-nucleon couplings are relatively model independent, they are undetermined to factors of order 1. Taking these and other concerns into account the authors of Ref. [16] estimate an uncertainty of a factor of 2 in their result, meaning the

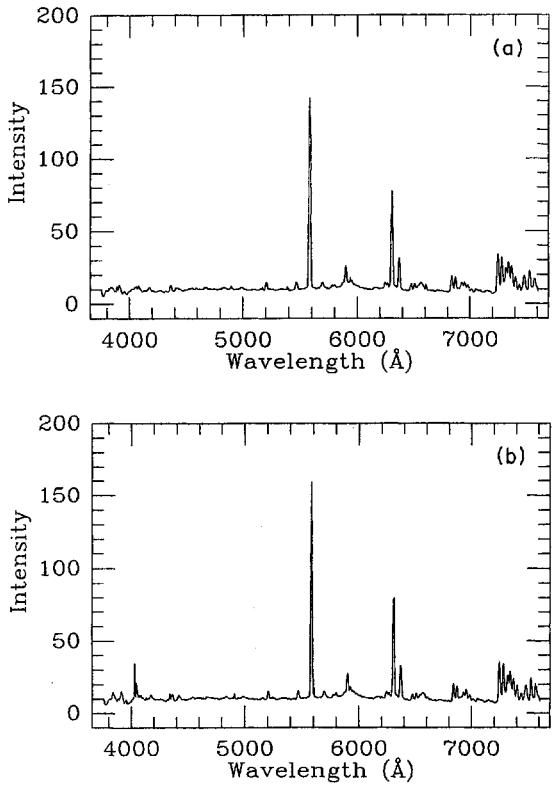

FIG. 4. Spectra of two intergalactic regions in the cluster A1413, night 2. (a) The inner, or "on," aperture ($R_a = 0.65$); (b) the outer, or "off," aperture ($R/a = 2.94$). Intensity is in units of 10^{-18} erg cm^{-2} arc sec^{-2} Å^{-1} sec^{-1}.

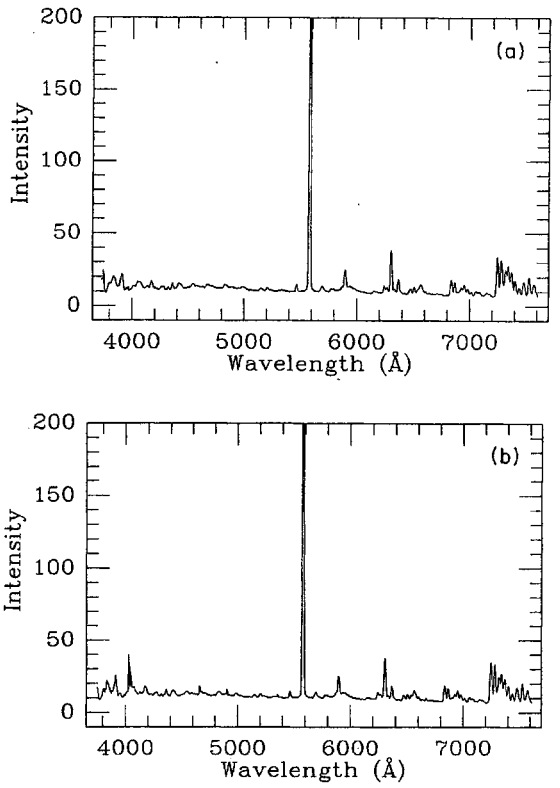

FIG. 5. Spectra of two intergalactic regions in the cluster A2218, night 2. (a) The inner, or "on," aperture ($R/a = 0.94$); (b) the outer, or "off," aperture ($R/a = 5.33$). Intensity is in units of 10^{-18} erg cm^{-2} arc sec^{-2} Å^{-1} sec^{-1}.

true lower bound to the window lies in the range 1.5 to 6 eV, with 3 eV being the probable value.

Stellar-evolution arguments provide one means of defining the upper bound to the multi-eV axion window. Raffelt and Dearborn [17] have considered the effects of hadronic axions upon various phases of a star's evolution (see also Refs. [18,20]). In their paper they derive two limits to the mass of the axion which are relevant to the present search. The first is $m_a \lesssim 2\zeta^{-1}$ eV from considering the effects of axion emission upon the peak brightness of RG stars at the tip of the giant branch. The second limit is even more restrictive, $m_a \lesssim 0.7\zeta^{-1}$ eV. This constraint derives from the fact that axions remove energy from the core of HB stars at a sufficient rate to shorten their calculated ages by a factor of 2. This would cause a discrepancy with the observed number of HB stars in the open star cluster M67. Both of these constraints seem to rule out the claimed existence of the multi-eV window (when combined with the results from the SN 1987A analysis), but there are at least two reasons to consider the window further.

Both of the above constraints depend upon the Primakoff effect for axion emission from the stars. This effect makes use of the same anomaly diagram which leads to the two-photon decay of the axion. Hence the same model dependence, as embodied by ζ, which enters the axion lifetime, plays a role here. In fact letting $E/N=2$ ($\zeta=0.07$), the above limits become $m_a \lesssim 30$ eV and $m_a \lesssim 10$ eV, respectively, well in excess of the lower bound from SN 1987A. We will find that we can do much better than this from considering relic decays. The other reason to consider the window further is simply that both of the above arguments are based upon the statistics of small numbers. Unlike the bound from SN 1987A, where the 19 observed neutrino events over about a dozen seconds trace the entire cooling history of the protoneutron star, RG and HB stars live for many millions of years. Thus, in order to infer the properties of RG and HB stars one must argue based upon the observed number of such objects as compared to other types of stars. In both of the above cases the data is a small sample which may, or may not, be statistically significant (in M67 there are only five HB stars). So, while the physics upon which the above two bounds are based seems quite sound, the observations are not yet at a level to confirm them.

Two recent analyses further complement the upper bound to this window. Haxton and Lee [18] have examined energy loss due to nuclear axion emission in RG and HB stars. Using criteria similar to that of Raffelt and Dearborn [17] they derive interesting upper limits to the mass of the axion. Since they consider nuclear emission, the model dependence embodied by ζ is not present. Unfortunately, this model dependence is replaced by a dependence on the strange-quark content of the nucleon, which has yet to be convincingly determined. Engel, Seckel, and Hayes [19] have used axion emission from SN 1987A to set another upper bound to this window of axion mass. By considering the effect of emitted axions upon the KII detector they have been able to exclude the existence of axions more massive than $\sim 5-10$ eV. While these axions would not seriously effect the energetics of the neutrino burst, they would interact with the target nuclei of the detector, causing an increase in the number of detected events. For masses above those mentioned, more events than were detected would be expected from axions alone, ruling out axions above this mass. Given the above possible loopholes, uncertainties in the stellar-evolution arguments, and the experimental uncertainties of the supernova limit, it makes sense to consider what other upper bounds one may derive to the mass of the axion. One possible method is to consider the effects of decaying axions upon the DEBRA.

Measurements of the DEBRA flux have, in several instances, been used to constrain the properties of neutrinos [22,23]. In much the same way these flux measurements can be used to constrain the properties of the axion [20]. If one makes the most conservative assumption, that axions are distributed uniformly throughout space, axions produce a diffuse glow in the night sky with an intensity of [12,23]

$$I_a = \frac{d\mathcal{F}_E}{dA\, d\Omega\, d\lambda\, dt} = \frac{n_a m_a c^3 (\lambda_a/\lambda)^3}{4\pi H_0 \tau_a \lambda_a [1-\Omega_{\rm tot}+\Omega_{\rm tot}(\lambda/\lambda_a)]^{1/2}} = \frac{n_a m_a c^3}{4\pi H_0 \tau_a \lambda_a}\left[\frac{\lambda_a}{\lambda}\right]^{7/2}, \qquad (4a)$$

valid for $\lambda > \lambda_a$, and where n_a = present axion number density, H_0 = the Hubble constant, λ = observed wavelength, $\lambda_a = 24\,800$ Å (eV/m_a), and $\Omega_{\rm tot} = \rho/\rho_{\rm crit}$ is the universal density parameter. The second step in Eq. (4a) follows from setting $\Omega_{\rm tot}=1$, the theoretically preferred value. It is interesting to note that if an axion with a mass of 6 eV or so was uniformly distributed throughout the cosmos, the spectral shape of the resulting glow might present a powerful method of determining $\Omega_{\rm tot}$. Unfortunately, as I will show, there is no such feature. From now on I will assume $\Omega_{\rm tot}=1$ and use the second expression in Eq. (4a).

If I now insert values of the quantities into Eq. (3), I find that an axion will produce a glow in the night sky of [12]

$$I_a\ (\lambda > \lambda_a) = 1.8\times 10^{-23}\left[\frac{m_a}{\rm eV}\right]^7 \frac{\zeta^2}{h_{50}}\left[\frac{15}{g_{*F}}\right]\left[\frac{\lambda_a}{\lambda}\right]^{7/2} \text{erg cm}^{-2}\,\text{arc sec}^{-2}\,\text{Å}^{-1}\,\text{sec}^{-1}, \qquad (4b)$$

where g_{*F} is the number of relativistic degrees of freedom when the axion freezes out (see the next section). Note that any limit to the axion mass derived from this will depend on $\zeta^{-2/7}$; this is a much weaker dependence than the stellar-evolution limits. It is now a simple matter to compare the flux predicted in Eq. (4) to that measured in DEBRA experiments.

There are numerous experiments which have searched

for and/or found the intensity of the DEBRA. For a recent review of the available data see Ref. [22]. I will focus on results which can be derived for axions with masses between 3 and 25 eV, the size of the window if we neglect the stellar-evolution arguments. There are a number of reasons for restricting ourselves to this region. First, SN 1987A precludes the existence of axions with $m_a < 3$ eV. Second, as I will show, no useful constraints on m_a may be derived from the DEBRA for $m_a < 3$ eV. Third, for $m_a > 25$ eV, τ_a is shorter than the age of the Universe and Eq. (4) is no longer valid. Lastly, for axion masses greater than about 25 eV the wavelength of the axion decay radiation is shorter than the Lyman limit, and a truly extragalactic flux cannot be measured due to the opacity of the interstellar medium. In this range I may now compare the intensity predicted by Eq. (4) to that actually measured. In Fig. 6 I present results of this exercise. I consider the intensity I_a for a number of axion masses and require a value of ζ small enough so that $I_a\ (\lambda=\lambda_a)=I_{\rm DEBRA}$. It is clear that throughout the region of interest ζ must be very small to be consistent with the observations. In fact, $\zeta=0.07$ $(E/N=2)$ occurs at an axion mass of 7.5 eV. This value of m_a constitutes the upper bound to the multi-eV window of axion mass. Figure 6 also clearly shows that as m_a approaches 3 eV, ζ goes to 1. The lowest value of m_a for which the available data gives any information is $m_a=3.8$ eV. For this mass $\zeta \leq 0.43$, so that in the simplest axion models consideration of the DEBRA flux requires $m_a \leq 3.8$ eV. This is still in excess of the SN 1987A bound.

The expected signal from axions residing in the halo of our Galaxy provides a complementary mass bound to that deriving from the DEBRA flux. This is because these two limits span a wide range of conditions from very clustered to totally unclustered. The galaxy analysis will thus strengthen the upper bound to the window of $m_a \lesssim 8$ eV.

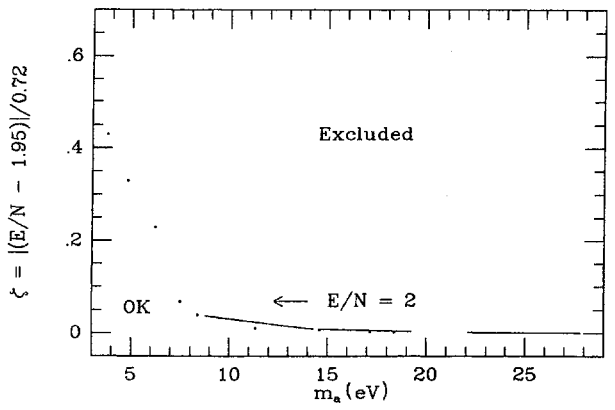

FIG. 6. Constraints to the parameter ζ obtained by considering the effects of the electromagnetic decay of unclustered axions upon the DEBRA.

The density of the galactic halo is usually parametrized as

$$\rho(r)=\rho_\odot \frac{R_\odot^2+a^2}{r^2+a^2}\ , \tag{5}$$

where $\rho_\odot$ is the local halo density, $R_\odot=8.5$ kpc is the distance from the Sun to the galactic center, and a is the halo core radius. Based upon galactic modeling, $\rho_\odot \simeq 5\times10^{-25}$ g cm$^{-3} \simeq 0.01 M_\odot$ pc^{-3} and the halo core radius lies between 2 and 8 kpc [24]. Note that for $r \gg a$, the density run of Eq. (5) is $\rho(r) \propto r^{-2}$, just as one would expect based upon the observed flat rotation curve of our Galaxy. The surface density observed in the model of Eq. (5) is $\Sigma(x,\theta)=R_\odot \rho_\odot J(x,\theta)$, where $x=a/R_\odot$, θ is the angle between the galactic center and the line of sight, and

$$J(x,\theta)=\frac{1+x^2}{\sqrt{x^2+\sin^2\theta}}\left[\frac{\pi}{2}+\arctan\left[\frac{\cos\theta}{\sqrt{x^2+\sin^2\theta}}\right]\right]. \tag{6}$$

Note that Eq. (6) can be rewritten in terms of galactic latitude and longitude (b,l) with the identification $\cos\theta=\cos b\cos l$. The next step is to determine what fraction of the halo's mass is made up of axions.

In clusters of galaxies I will argue that the axion mass fraction should be $\geq \Omega_a$. This is not the case in the halo of our Galaxy. In our halo, phase-space arguments similar to those proposed by Tremaine and Gunn [25] play an important role in limiting the axion density. (I will discuss this point in detail in the next section; see also Ref. [26].) Inserting the central halo density implied by Eq. (5) into Eq. (12a), the axion mass fraction is seen to obey

$$r_a(\max)\simeq 1.1\times10^{-6} g_a \left[\frac{m_a}{\rm eV}\right]^4 \sigma_2^3 \frac{x^2}{1+x^2}\ , \tag{7}$$

where the halo velocity dispersion is $\sigma=\sigma_2\times100$ km sec^{-1}. $r_a(\max)$ is much less than Ω_a, implying a much weaker signal than for clusters of galaxies. [As I will show later, the Bose-Einstein nature of axions will do little to change r_a. Furthermore, since $m_a \propto I_a^{1/10}$, an uncertainty in $r_a(\max)$, which itself varies as m_a^4, of even a factor of 10 will not significantly affect the conclusion.] Making the identification $\Sigma_a=r_a(\max)\Sigma$ and using expressions derived in Sec. III leads to the conclusion that axions in our halo should produce an emission line at a wavelength of $\lambda_a=24\,800$ Å (eV/m_a), with a width of ~ 20 Å $\sigma_2(\mathrm{eV}/m_a)$, and with an intensity of

$$I_a^{\rm halo}(R,\lambda)=1.7\times10^{-25}\left[\frac{m_a}{\rm eV}\right]^{10} \times\zeta^2\sigma_2^2 G(x,\theta)\exp\left[\frac{-(\lambda-\lambda_a)^2}{\lambda_a^2}\frac{c^2}{2\sigma^2}\right] \tag{8}$$

in units of erg cm^{-2} arc sec^{-2} Å^{-1} sec^{-1}. Here I have defined $G(x,\theta)=x^2/(1+x^2)J(x,\theta)$. The function $G(x,\theta)$ varies between about 0.1 and 1 for reasonable choices of x $(\frac{1}{4} \lesssim x \lesssim 1)$.

The most simple-minded limit which can be derived

from Eq. (8) is obtained by requiring that $I_a^{\rm halo}$ not exceed the continuum level of the night sky ($I_{\rm NS}\sim 10^{-17}$ erg cm^{-2} arc sec^{-2} Å^{-1} sec^{-1}). Assuming $x\simeq 1$ ($G\simeq 1$), I find the very conservative bound $m_a \lesssim 6\zeta^{-1/5}$ eV from the halo of our Galaxy. Any axion more massive than this would create a line in the spectrum of the night sky which could not have escaped notice. Thus, as claimed, the signal which would arise from axions in our halo complements the bounds arising from the DEBRA measurements.

Astrophysics and cosmology have provided several convincing ways of constraining the axion mass to delineate the 3–8 eV axion window. The lower bound is placed by considerations of the neutrino burst of SN 1987A. This burst also helps to set the upper bound to the window. Stellar-evolution arguments may have already closed the window, but this is far from certain. The relic decays of highly clustered and unclustered axions provide a complementary, and conservative, probe to the upper bound of the window. Both of these methods of constraining the axion mass share a dependence upon the axion model. But even in the worst-case scenario $E/N=2$ relic delays still constrain the axion to be less massive than about 8 eV. This constitutes the claimed upper bound to the axion window. In the remainder of the paper I will describe an attempt to probe this window using the decays of axions residing in clusters of galaxies.

III. AXIONS IN CLUSTERS

In order to search for relic axions in clusters of galaxies it is important to carefully determine how the axion signal will manifest itself. To do this one must determine the abundance of axions in the cluster, how they are distributed, the shape of the line, and several other points. In this section I will address these issues and derive expressions for the expected signal from axion decay in clusters of galaxies.

The first step in determining the axion abundance in clusters of galaxies is to find their universal abundance. (This was important in deriving the previous bounds to the axion mass from the DEBRA flux. In this argument I adopt high-energy physics units $\hbar=c=k_B=1$). As mentioned above, axions with masses greater than 10^{-2} eV are thermally produced [10,12]. The relevant process for creating a thermal population of axions is axion-pion conversion: $N+\pi\rightarrow N+a$, where N is a nucleon of mass $m_N=939$ MeV. The reaction rate for this process is roughly given by

$$\Gamma=n_N\langle\sigma|v|\rangle\sim(T^3/m_\pi^2)[m_N/(f_{\rm PQ}/N)]^2 \times(m_N/T)^{-3/2}\exp(-m_N/T)\ .$$

The rate to compare this with is the expansion rate $H=1.66g_*^{1/2}T^2/m_{\rm Pl}$, where $m_{\rm Pl}$ is the Planck mass and g_* is the number of relativistic degrees of freedom [27]. When $\Gamma/H\gtrsim 1$ for an expansion time ($\sim 1/H$) axions thermalize. The ratio of the two rates is

$$\frac{\Gamma}{H}\sim 10^8\left[\frac{m_a}{\rm eV}\right]^2\left[\frac{m_N}{T}\right]^{-3/2}\exp(-m_N/T)\ . \qquad (9)$$

For axions with masses of several eV, Γ/H is larger than 1 for temperatures above 50–60 MeV. Thus at temperatures above 60 MeV axions are in thermal equilibrium. (Note: The above expression is only valid for temperatures $T\lesssim T_{\rm QH}\sim\Lambda_{\rm QCD}\simeq 150$–$400$ MeV. This is the temperature of the quark-hadron phase transition, and before this time there are no nucleons or pions to interact with. Axions will likely be in equilibrium above this temperature due to their interactions with quarks, but here we are only interested in their freeze-out temperature which lies below $T_{\rm QH}$.) At temperatures below 50 MeV the axion abundance freezes in at a value of $n_a=[\zeta(3)/\pi^2]T_a^3$, where T_a is the axion temperature. This corresponds to a present-day axion number density of

$$n_a\simeq 55\ {\rm cm}^{-3}\left[\frac{15}{g_{*F}}\right], \qquad (10)$$

where g_{*F} is the number of relativistic degrees of freedom when axions froze out at $T\sim 50$ MeV. At temperatures of ~ 50 MeV the average energy per particle is $\sim 3T=150$ MeV; thus the particles which should still be relativistic are the $\pi^\pm$, π^0, $\mu^\pm$, $e^\pm$, $\nu_{e,\mu,\tau}$, $\bar\nu_{e,\mu,\tau}$, γ, and a. Naively summing these degrees of freedom results in $g_{*F}=18.75$. This is not quite correct, since both the pions and the muons are becoming nonrelativistic at this temperature. The result of a numerical integration [27] gives $g_{*F}\simeq 15$, the value I use throughout. This can easily be converted into a mass density and thence to a fractional density of the Universe,

$$\Omega_a h_{50}^2=\frac{1}{49}\left[\frac{m_a}{\rm eV}\right]\left[\frac{15}{g_{*F}}\right] \qquad (11)$$

and $H_0=50h_{50}$ km/sec Mpc^{-1}. Equation (11) shows that the axions in the multi-eV window cannot be the dark matter which seems to pervade the Universe, but that they do contribute an amount of density comparable to that of baryons. Having determined Ω_a it is now important to determine what fraction of the galaxy cluster's mass could be in axions.

Axions, along with baryons and any other nonrelativistic particles, should participate in the collapse which forms clusters of galaxies. The equivalence principle ensures that the ratio of the axion number density to the number density of all species which collapse into the cluster should remain constant. This leads to the relation that $\rho_a=(\Omega_a/\Omega_{\rm cluster})\rho_{\rm cluster}$, where ρ_a is the mass density in axions, $\rho_{\rm cluster}$ is the mass density of all matter in the cluster (which is determined observationally), and $\Omega_{\rm cluster}$ is the fractional density of all matter that falls into the cluster. Since baryons are known to exist and should collapse, we know that $\Omega_{\rm cluster}\geq\Omega_a+\Omega_B$. An upper bound to $\Omega_{\rm cluster}$ is $\Omega_{\rm cluster}\leq\Omega_{\rm tot}=1$. Thus, the density of axions in the cluster lies between the values $[\Omega_a/(\Omega_a+\Omega_B)]\rho_{\rm cluster}\geq\rho_a\geq\Omega_a\rho_{\rm cluster}$. Combining this argument with the well-known bounds from primordial

nucleosynthesis [28], $0.044 \gtrsim \Omega_B h_{50}^2 \gtrsim 0.15$, we find that the axion density lies in the range $10\Omega_a \rho_{\rm cluster} \gtrsim \rho_a \gtrsim \Omega_a \rho_{\rm cluster}$ for all axion masses in the multi-eV window. I shall use the most conservative assumption throughout the rest of the discussion, $\rho_a = \Omega_a \rho_{\rm cluster}$, but it bears remembering that this may underestimate the number of axions in the cluster by up to a factor of 10.

A possible loophole in the above discussion, which would tend to lower the number of axions in the cluster, is the question of available phase space. Once axions decouple from the plasma, their microscopic phase-space density is conserved (i.e., they obey the collisonless Boltzmann equation $df/dt = 0$). For a thermal distribution of axions the initial phase-space occupancy is $\lesssim 1$ per cell of phase space for the great majority of axions. This is easily demonstrated: axions obey Bose-Einstein statistics. The axion distribution function is then $f(E) = (e^{E/T} - 1)^{-1}$ ($\hbar = c = k_B = 1$), which is greater than one for $E \leq E_* = \ln(2) T$. The number density of axions with energies less than or equal to E_* is

$$n\ (<E_*) = \frac{g_a}{2\pi^2} \int_0^{E_*} \frac{E^2 dE}{e^{E/T} - 1}\ ,$$

where I have neglected m_a (which is certainly valid at the decoupling temperature of ~ 50 MeV). For $E/T < 1$ the exponential in $n\ (<E)$ can be expanded with the result that

$$n\ (<E) \simeq (g_a T/2\pi^2) \int_0^E E\, dE = (g_a T/2\pi^2) E^2\ .$$

This can be rewritten as

$$n\ (<E) \simeq [2\zeta(3)]^{-1} (E/T)^2 n_a \simeq [2\zeta(3)]^{-1} f(E)^{-2} n_a\ ,$$

valid for $E < T$. We see that the number of axions which have phase-space densities greater than 1 is suppressed by a factor of $(E/T)^2$ at decoupling and that the larger the phase-space occupancy, the smaller the number of axions with that occupancy. As an example of this, the above shows that the number density of axions with $f(E) \geq 1$ is $\sim 0.2 n_a$, or only about 20% (see also Ref. [26]). Carrying this even further, the percentage of axions with a phase-space density greater than 10/cell is only 0.3%. Furthermore, during the collapse of the cluster, or galaxy, dynamical processes such as phase mixing and violent relaxation are likely to reduce the phase density if they affect it at all [29,30].

Since there is only a small fraction of the axions in high occupancy states and the phase-space density is conserved, the arguments of Tremaine and Gunn [25] apply to thermal axions as well as to neutrinos. Assuming a phase-space density of 1 and applying their argument to axions, I find that the maximum axion mass fraction in a cluster based upon the available phase space, $r_a(\max)$, is

$$r_a(\max) = \frac{(2\pi)^{3/2} g_a m_a^4 \sigma^3}{h^3 \rho_c}\ , \qquad (12a)$$

where $\sigma = \sigma_3 \times 10^3$ km sec^{-1} is the one-dimensional cluster velocity dispersion and ρ_c is the central density of the cluster. Going a step further and assuming that the cluster core is described by an isothermal sphere distribution or the analytic King model (to be described shortly), we can use the relation $\rho_c = 9\sigma^2/4\pi G a^2$ to rewrite this as

$$r_a(\max) = \frac{2(2\pi)^{5/2} g_a G a^2 \sigma m_a^4}{9h^3}$$
$$\simeq 3 \times 10^{-3} g_a \left[\frac{m_a}{\rm eV}\right]^4 \sigma_3 a_{250}^2\ , \qquad (12b)$$

where $a = a_{250} h_{50}^{-1} \times 250$ kpc is the cluster core radius. It is clear from the above discussion that the Bose character of the axion will not increase r_a by very much. For axions with masses in the multi-eV window, with typical cluster parameters ($a_{250} = \sigma_3 = 1$), $r_a(\max) \gtrsim 1 \gg \Omega_a$. There is plenty of phase space for the axions in clusters of galaxies. This was not the case when we considered axions in the halo of our Galaxy. In that case Eq. (7) or a similar constraint plays a very important role in determining the axion signal.

Thermal axions become nonrelativistic when $T_a \simeq m_a/3 \sim 1$ eV, before the time of matter-radiation decoupling ($1 + z_{\rm dec} \simeq 1150$). Momentum, and hence velocity, are proportional to $(1+z)^{-1}$ for nonrelativistic particles. Thus, unclustered axions should be characterized by a velocity dispersion of order

$$\langle v_a^2 \rangle^{1/2} = v_a \simeq 4.3 \times 10^{-4} c (\text{eV}/m_a)(15/g_{*F})^{1/3}$$

today. The requirement that axions collapse with the perturbations that form clusters (i.e., that the axion Jean's mass is small enough) is simply that $v_a \lesssim \sigma_{\rm 3D}$, the three-dimensional cluster velocity dispersion, at the time of cluster formation. This requirement is amply met for cluster formation redshifts smaller than 15 or so. Thus, as claimed, there is every reason to expect that axions will collapse with other matter into clusters of galaxies.

As the axions collapse, how will they distribute themselves in the cluster? The process of violent relaxation will tend to produce a Maxwellian velocity distribution [29–31]. Since this is the distribution function of an isothermal sphere, one would expect the corresponding density profile. Numerical N-body experiments generally show that during collapse a gas of dissipationless particles does not completely relax to the isothermal profile. The relaxed configurations are not too different from an isothermal sphere, and this remains a useful approximation to the density profile [32,33]. (In fact, N-body simulations of cluster formation and relaxation result in profiles very similar to the analytic King, or modified Hubble, profile which I shall use to model clusters [29,31,33].) This picture is further borne out by observations of clusters themselves. Since clusters as a whole, as opposed to the individual galaxies within them, appear to have undergone little dissipation, the light should trace the mass in these objects; in any case, it should trace the gravitational potential well. It should then be possible to use both the galaxy and x-ray gas distributions to investigate the axion distribution. Observations reveal that the density distribution of the isothermal sphere and various approximations to it seem to provide an excellent

description of the available data [31].

A number of density profiles have been successfully fit to the distributions of galaxies and x-ray gas in clusters [29,31]. Among the most successful of these is the profile

$$\rho(r)=\frac{\rho_c}{(1+r^2/a^2)^{3/2}}\ , \tag{13}$$

where ρ_c = the central density of the cluster, r = the radial distance from the cluster center, and a is the cluster core radius. This is often referred to as the analytic King (AK) model. The AK model has several desirable features beyond its ability to fit the data. As its name implies, it gives simple analytic formulas for all of the relevant observables. It is also a fairly accurate representation of an isothermal sphere for $r \lesssim$ several a (the region where most of our data was acquired) and has a central density determined by observable quantities in the cluster,

$$\rho_c=\frac{9\sigma^2}{4\pi G a^2}\ , \tag{14}$$

where σ is the one-dimensional velocity dispersion of the cluster. Another profile which is often used to model clusters is

$$\rho(r)=\frac{\rho_c}{1+r^2/a^2}\ . \tag{15}$$

This is a better fit to an isothermal sphere distribution in the outer regions of the cluster, but at the expense of the inner regions. When comparing the observations to the data, I have considered both of the above models. In this paper I will limit the discussion to the AK model, with only cursory comments about the model of Eq. (15), for two reasons: (1) the AK model of Eq. (13) seems to be slightly more successful in modeling clusters than the other distribution, and (2) in the region which the observations cover, there is not a large difference in the predicted axion decay intensity between the two models. I obtain more conservative bounds using the AK model. Thus, any statement made concerning the axion based upon the AK model will only be stronger in the model of Eq. (15).

Having decided upon a density profile to describe the cluster, and hence the axion distribution in the cluster, the last ingredient needed to find the axion signal in a cluster is the line shape. Particles in the cluster are generally taken to be distributed with a Maxwellian (Gaussian) velocity distribution [31]

$$\mathcal{P}(v_r)dv_r=\frac{1}{\sigma\sqrt{2\pi}}\exp[-(v_r-\langle v_r\rangle)^2/2\sigma^2]\,dv_r\ , \tag{16}$$

where v_r is the measured velocity projected along the line of sight (recessional) of the particle (i.e., galaxy) in the cluster. Here $\mathcal{P}(v_r)dv_r$ is the probability that an individual particle has a line-of-sight velocity in the range v_r to v_r+dv_r. This is easily converted into a probability distribution for λ using the nonrelativistic Doppler formula $\Delta\lambda/\lambda=v/c$ with the result

$$\mathcal{P}(\lambda)d\lambda=\frac{c}{\sqrt{2\pi}\sigma\lambda_a}\exp\left[-\frac{(\lambda-\lambda_a)^2}{\lambda_a^2}\frac{c^2}{2\sigma^2}\right]d\lambda\ . \tag{17}$$

Equation (17) (without the $d\lambda$) is the profile of the line. For future reference, Eq. (17) describes a line with a Gaussian profile and a full-width at half-maximum (FWHM) of $\Delta\lambda_{\rm FWHM}=2\sqrt{\ln 4}(\sigma/c)\lambda_a\simeq 2.4(\sigma/c)\lambda_a$.

It is now straightforward to predict the expected intensity of an axion decay line as a function of λ, projected cluster position, and axion mass. The first thing to do is to integrate along the line of sight through the cluster to obtain the surface density $\Sigma(R)$. Using the AK model the surface density is

$$\Sigma(R)=\frac{2\rho_c a}{1+R^2/a^2}\ , \tag{18}$$

where R is the projected radial distance from the cluster center. As per the discussion above, the axion surface density is $\Sigma_a(R)=\Omega_a\Sigma(R)$. With this identification the predicted axion signal becomes

$$I_a(R,\lambda)=\frac{d\mathcal{F}_E}{dA\,d\Omega\,d\lambda\,dt}=\frac{\Sigma_a(R)c^2\mathcal{P}(\lambda)}{4\pi\tau_a}\ . \tag{19a}$$

Combining Eqs. (2), (11), (14), (17), and (18) and putting in numbers this becomes

$$I_a(R,\lambda)=6.9\times10^{-21}\left[\frac{m_a}{\rm eV}\right]^7\left[\frac{\sigma_3}{h_{50}a_{250}}\right]\left[\frac{15}{g_{*F}}\right]\times\zeta^2\exp\left[\frac{-(\lambda-\lambda_a)^2}{\lambda_a^2}\frac{c^2}{2\sigma^2}\right]\Big/\left[1+\frac{R^2}{a^2}\right], \tag{19b}$$

in units of erg cm^{-2} arc sec^{-2} Å^{-1} sec^{-1}. Equation (19) describes an axion decay line, in the cluster rest frame, which is centered at a wavelength $\lambda_a=24\,800$ Å (eV/m_a) and a FWHM of $\sim$200 Å σ_3(eV/m_a). In our rest frame the line center is shifted to $\lambda_a\Longrightarrow\lambda_a(1+z)$ and the width is broadened by a factor of $1+z$ as well. These two considerations will help to distinguish candidate axion lines from night sky lines. Finally, in our frame, I_a suffers from a cosmological dimming which further reduces the flux by a factor of $(1+z)^{-4}$. Important features to note about Eq. (19b) are the spatial dependence of the line strength ($\propto R^{-2}$ for $R>a$), its dependence upon ζ^2, and the strong dependence on m_a (to the seventh power). The dependence of $I_a\propto\rho_a/\lambda_a\tau_a$ upon m_a is easily understood, m_a^5 from τ_a, m_a from $\rho_a\propto\Omega_a$, and m_a from λ_a. Had we used the density profile of Eq. (15), the main difference would have been in the spatial dependence $I_a\propto 1/R$ for $R>a$.

Now that we have a prediction for the axion signal, we can design a search which will optimize the chance of detecting this feature. Neglecting the line shape, and much of the parameter dependence, Eq. (19b) can be rewritten as

$$I_a\simeq 1.5\times10^{-17}(m_a/3\ {\rm eV})^7\times\zeta^2/(1+R^2/a^2)\ {\rm erg\,cm^{-2}\,arc\,sec^{-2}\,Å^{-1}\,sec^{-1}}\ .$$

Thus an axion in the lower end of the mass window has a predicted intensity comparable to that of the night sky continuum ($I_{NS} \sim 10^{-17}$ erg cm^{-2} arc sec^{-2} Å^{-1} sec^{-1}). Furthermore, there are numerous strong emission lines through the relevant spectral range ($\sim$3000–8500 Å) [14]. This problem is especially acute towards the red end of the spectrum (corresponding to small axion masses and hence to small I_a) where there are numerous emission bands from molecular OH (see Figs. 1–5). In order to secure an unambiguous detection of an axion line, especially in the case of $\zeta < 1$, the night sky background must be removed. Fortunately, the spatial dependence of Eq. (19) suggests an easy solution. By taking a spectrum from near the cluster center, where the line is strongest, and subtracting from it a spectrum taken from the outskirts of the cluster ($R > 2a$), the night sky may be removed with very little effect upon the axion line. In principle, this procedure should allow the entire window to be easily probed. In practice, there are several complications. Foremost among these is the fact that the night sky varies both spatially and temporally, making a perfect subtraction impossible. In order to achieve the best subtraction possible one should take the spectra as close together in space and time as possible. When this is done, intensities of between 1 and 10% of the night sky continuum are typically achieved. Another worry is that the axion distribution may be more diffuse than the baryon distribution (e.g., $a_{\text{axion}} \gg a_{\text{galaxies}}$) and the subtraction procedure may remove the line. I will address this concern in the next section.

A search for an axion decay line in three well-studied clusters of galaxies, A1413, A2218, and A2256, was carried out in May 1990 [15]. These three clusters have a number of properties which make them ideal for a search of this type. Each of these clusters has been extensively studied at both optical and x-ray wavelengths. Thus, the cluster parameters such as the core radius a and the velocity dispersion σ are fairly well determined. They are quite rich clusters with well-determined centers; each has a fairly large velocity dispersion, meaning a large mass and therefore a potentially stronger axion signal. Another advantage of these clusters is their distance from us. Each is distant enough so that the cluster is reasonably small on the sky, $\sim$5 arc min, yet not so far away that candidate axion lines are shifted too far into the red or dimmed by too great a factor. Additionally, they span enough of redshift space so that if the axion line falls in a region of poor night sky subtraction in one cluster's spectrum, it should fall in a region of good subtraction in another's spectrum. Table I summarizes the relevant parameters of the three clusters. There is some scatter in the data, so in choosing the values of a and σ to use in Eq. (19) I have chosen representative and convenient values which agree with most of the data. For the actual data see Refs. [34], [35], and [36] for the clusters A1413, A2218, and A2256, respectively.

Before proceeding to describe the observations of these clusters, I will discuss a final issue which bears upon the multi-eV window. Now that we have a firm prediction of the intensity of an axion decay line in a cluster of galaxies, we can ask if any previous searches for intracluster light might have detected it. The answer turns out to be "yes" for a range of mass both within and outside of the window. In the ultraviolet region there are two spectroscopic observations of the Coma cluster of galaxies which clearly rule out axions in the mass ranges 16–20 eV and 22.1–27.8 eV for any plausible value of ζ [37]. As support for this statement I consider the data of Henry and Feldman [37] at 1300 Å ($m_a = 19.5$ eV). Their upper limit to any line flux in the Coma cluster at this wavelength is $I_{\text{line}} \lesssim 1.4 \times 10^{-19}$ erg cm^{-2} arc sec^{-2} Å^{-1} sec^{-1}. For an axion decay line with $\zeta = 1$, Eq. (19b) predicts $I_a \simeq 1.7 \times 10^{-12}$ erg cm^{-2} arc sec^{-2} Å^{-1} sec^{-1}; a flux of more than 1.0×10^7 times that measured. This strongly demonstrates the strong dependence of I_a upon the axion mass. To hide such a line in Coma, one needs $\zeta \leq 0.0003$, requiring a near miraculous cancellation to the two amplitudes which lead to axion decay. Of more interest are two sets of broadband searches for intracluster light performed in the optical [38]. Shipman and Cowsik [38] used a number of pre-existing observations of intergalactic light to set constraints upon the lifetime of the neutrino to radiative decay. Their limits may easily be translated to limits on m_a via a modified Eq. (19). Since the observations are broadband, they only measure the total flux in the band; all wavelength information is lost. It is simple to predict the total flux produced by an axion line in a band; simply integrate Eq. (19) over the wavelength λ. This has the effect of making the function $\mathcal{P}(\lambda)$ become 1 with the corresponding change in I_a. When this is done, the g- and r-band observations used by Shipman and Cowsik rule out the standard ($\zeta = 1$) axion in the range 5.4–3.6 eV. The work of Partridge and collaborators [38] is similar but probes further into the red. Unfortunately, due to problems with the data it is uncertain how to convert their data into constraints on m_a. Previous data place interesting limits upon m_a but do not close the axion window. Furthermore, these limits are difficult to turn into convincing constraints on ζ; this is much simpler for spectroscopic observations, such as those I will describe shortly.

TABLE I. Summary of properties of the three clusters observed.

Cluster	σ (km sec^{-1})	a kpc (arc min)	z
A1413 [34]	1230	$400h_{50}^{-1}$ (2.03)	0.1427
A2218 [35]	1300	$200h_{50}^{-1}$ (0.88)	0.171
A2256 [36]	1300	$473h_{50}^{-1}$ (5.0)	0.0601

IV. THE OBSERVATIONS

Long slit spectroscopic observations of the clusters A1413, A2218, and A2256 were obtained on the nights of 24 and 25 May 1990 at KPNO. The 2.1-meter telescope was used with the Gold Camera CCD spectrograph at a resolution of $\sim$10 Å. This resolution is well matched to a cluster axion line which would have a FWHM of about

$200\sigma_3$ Å (eV/m_a) in the three clusters. The incoming light passes through a 5′ by 2″.5 slit onto the grating of the spectrograph which then disperses the light onto 480×800 pixels of the CCD. Each exposure contains both spatial (480 pixels at 0″.78/pixel) and spectral (800 pixels at 4.6 Å/pixel) information. Pixels were binned by three in the spatial direction to increase the signal-to-read-noise ratio in the CCD. Thus, there are 160 individual spectra per slit position, each sampling a different spatial point in the cluster. On the first night we took multiple exposures of all three clusters using KPNO Gold Camera grating No. 400. This grating allowed observations in the wavelength range 4762–8441 Å, corresponding to axion masses in the range 6.1–3.2 eV when redshift effects are taken into account. For each cluster we walked the slit from a position near the cluster core to the cluster outskirts along an E-W axis, obtaining spatial information out to between 3 and 10 core radii for each cluster. Thus, if there were an axion line present, its spatial profile could be determined. This would help to confirm the line as arising from axion decay as well as provide valuable information about the cluster potential. On the second night grating No. 201 was used, which allowed a wavelength coverage of 3737–7606 Å (axion masses from 7.8–3.7 eV, including redshift), to observe the two smaller clusters (A1413 and A2218). Here single exposures were taken of each cluster as the 5′ slit covered more than 3 core radii for each. The exposure times ranged from 30 to 75 min/(slit position) and were chosen to ensure a large signal-to-noise ratio for the postulated axion line (see Table II for observing information).

The data were reduced using the Image Reduction and Analysis Facility (IRAF) version 2.8 as supplied by KPNO. The CCD bias was subtracted from each frame, and spatial variation in the pixel response and illumination were removed by dividing each spectrum by dome and sky flats taken earlier in the evening. Calibration in the spectral dimension was obtained by exposures of a He-Ne-Ar lamp. Observations of a KPNO standard star [39] (Wolf 1346) provided absolute flux calibrations for all exposures.

In Figs. 1–5 I present the spectral data used in the search for an axion decay line. Figures 1–3 are from the first night's observations and 4 and 5 are from the second night. In each of these sets of data (a) is the inner aperture, or "on-cluster" data. The on-cluster data is the spatial average of 30 pixels (23″.4) from near the cluster core, $R/a \lesssim 1$. Part (b) of each figure is the "off-cluster" data. The off-cluster spectra are the average of 30 pixels well away from the cluster center, $R/a \gtrsim 3$. Comparing Figs. 1–5 it is immediately apparent that all of the spectra are basically similar; they are simply spectra of the night sky. General features worth noting are the relatively constant continuum level of $I_{\rm NS}\sim10^{-17}$ erg cm^{-2} arc sec^{-2} Å^{-1} sec^{-1} and the numerous emission lines and bands which stand high above the continuum level and vary in intensity from spectrum to spectrum. No line which meets the criteria for an axion decay line, set out below, is in evidence. To lessen the chance of inadvertently removing a candidate axion line, cosmic-ray hits on the CCD have not been removed. These hits are easily distinguished on an individual basis as they meet none of the criteria which define an axion line. The bright level of the continuum and the many lines could very well overwhelm, or mimic, a candidate cluster emission line, so it is advantageous to remove them as well as possible. This is accomplished by subtracting the off-cluster spectrum of (b) from the on-cluster spectrum of (a). The resulting "on-off" spectra are shown in Figs. 7(a)–(e). This procedure should efficiently remove the night sky and, by virtue of the spatial dependence of the axion line [see Eq. (19)], scarcely affect any cluster emission line at all.

The most striking fact about the on-off spectra in Fig. 7 is the quality of the subtraction. Intensity levels of 1–10% of the continuum night sky level are easily achieved, except in the very brightest of the night sky emission lines. Furthermore, there appears to be little or no offset of the subtracted spectra in Fig. 7 from the value of 0, again indicating the quality of the subtraction. The best subtraction achieved is that in Fig. 7(b), A2218 on night 1. Because of the relative smallness of the cluster, $a=0'.88$, compared to the size of the slit, $\sim5'$, both the on-cluster and the off-cluster spectra came from the same observation, eliminating the temporal variation of the night sky. This spectrum has several features which occur in all of the on-off spectra and so deserves a bit of

TABLE II. Summary of information concerning the observations of the three clusters: exposure time is per slit position, if more than one slit position was observed for a cluster the slits lie on the East-West axis with the slit centers separated by 253″, night 1 refers to 24 May and night 2 to 25 May.

Cluster	Mass range (eV)	Exposure time (sec)	Inner aperture (R/a)	Outer aperture (R/a)	Number of slits	Night
A1413	3.36–5.95	2700	1.11	4.64	3	1
	3.73–7.58	4500	0.65	2.94	1	2
A2218	3.44–6.1	2700	0.94	5.33	2	1
	3.82–7.77	4500	0.94	5.33	1	2
A2256	3.11–5.52	1800	0.484	2.96	3	1

discussion. While in general the subtractions seem to be quite successful, there appear to be a number of residual lines. Might these be the result of axion decay? For this spectrum, and all of the others, the answer is "no"; all of the residual lines fail to meet the axion line criteria. In Fig. 7(b) the two lines, one positive, one negative, at $\lambda = 5035$ and 5350 Å are cosmic-ray hits. The features at 5577 Å and to the red of 7500 Å are due to poor night sky subtraction in the bright emission lines (and bands). These features are endemic to all of the spectra and each must be checked individually. One last point to note about the spectra in Fig. 7 is the relatively large amount of noise in the blue portion of the second night's data. This is due to too little flux reaching the pixels in our dome flats in the blue end of the spectrum (the spectrograph's efficiency drops rapidly for short λ). This noise turns out not to be a problem because of the strong dependence of I_a on m_a ($I_a \propto m_a^7$). Any line in this part

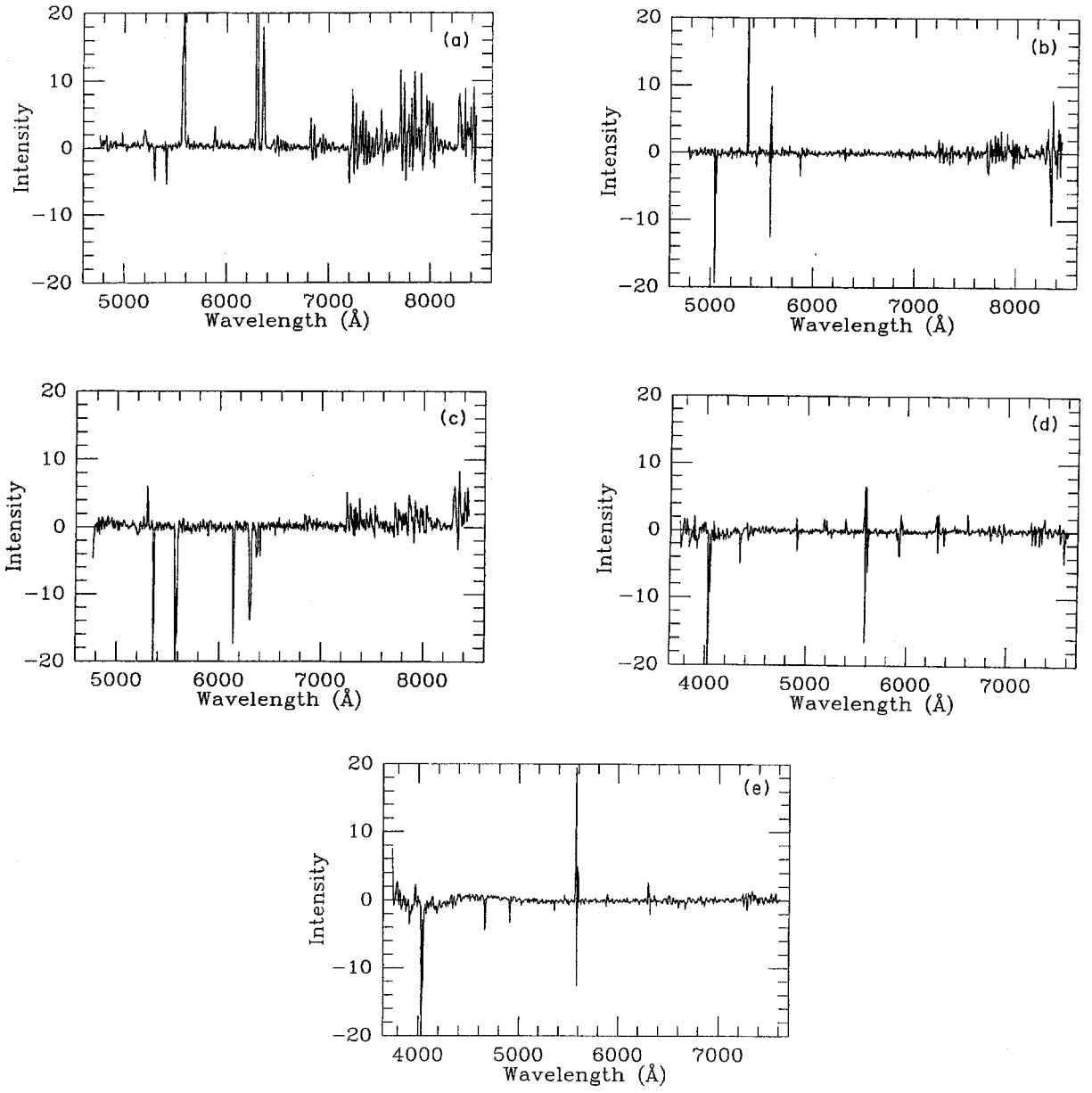

FIG. 7. The on-off spectra corresponding to Figs. 1–5. In each of these figures the spectrum in part (b) has been subtracted from the spectrum in part (a). Cosmic-ray hits and poorly subtracted night sky lines have not been removed. (a) A1413, night 1; (b) A2218, night 1; (c) A2256, night 1; (d) A1413, night 2; (e) A2218, night 2. Intensity is in units of 10^{-18} erg cm^{-2} arc sec^{-2} Å^{-1} sec^{-1}.

of the spectrum would stand far above the noise for any reasonable value of ζ.

What criteria must a candidate line in the spectra of Figs. 1–5 and 7 meet before it can be seriously considered as being from axion decay? First, each of the clusters should show a line that has been redshifted from a common rest wavelength. Next, the line should have approximately the predicted intensity, Eq. (19), and be Doppler broadened to a Gaussian with a FWHM of $\Delta\lambda/\lambda = 2\sqrt{\ln 4}\sigma/c$. Finally, the line should have a reasonable spatial profile (i.e., follow the AK or some similar model). In addition to using the data in Figs. 1–5 and 7, this could be checked by examining spectra from apertures between the two already examined. This would not only be a useful check on whether the candidate line could be from axion decay; it could also yield interesting information on the cluster potential. While these criteria are not enough to make the case for an axion decay line with certainty (e.g., an intracluster atomic emission line could easily satisfy all of the requirements), any line meeting them would certainly bear closer scrutiny by other methods (e.g., a proposed axion-photon conversion experiment which could detect solar axions in the range $0.1 \lesssim m_a \lesssim 5$ eV [40]). Naturally the converse is true; any line not meeting these requirements can be discarded from consideration.

The simplest way to check for the presence of an axion line in the data is to compare the real data of Fig. 7 to data with an artificial line, which obeys Eq. (19), inserted into it. In Fig. 8 I show several spectra with axion decay lines which arise from axions of different mass. Figure 8(a), when compared with Fig. 7(c), illustrates the major result of this paper: that there is no intracluster line emission from axion decay for axions with $m_a > 3.2$ eV. Figure 8(a) is the on-off ($R/a = 0.48$ minus $R/a = 2.96$) spectrum of A2256 with a 3.2-eV axion line artificially introduced. The line is at a central wavelength of $\lambda = \lambda_a(1+z) = 8216$ Å with a FWHM of ~ 80 Å and an intensity given by Eq. (19b) (with $\zeta = 1$). The axion line is the most obvious feature in the spectrum and is easily identifiable, in spite of the fact that it lies in the noisy, red portion of the spectrum. Since $I_a \propto m_a^7$, any line from a more massive axion would stand out far more prominently. A2256 has the lowest redshift of the three clusters surveyed and hence probes the lowest range of axion mass; Fig. 8(a) represents the lower bound to the axion mass from this search: $m_a < 3.2$ eV. The remainder of the data will serve to confirm this result, as well as exclude the presence of an axion with $m_a < 7.8$ eV. In Fig. 8(b) I have placed a 3.5-eV axion decay line in the night 1 spectrum of A2218, and in Fig. 8(c) a 6.5-eV line in the night 2 spectrum of A2218. This latter figure should be compared to the spectra of Fig. 5; a line this intense would stand far above the continuum in the unsubtracted spectra as well. The important point to notice in these figures is the strength of the line compared to the zero level of the subtraction. Such lines are clearly not present in any of the spectra of Fig. 7. The final result of these comparisons is that an axion with a mass in the range $3.2 \lesssim m_a \lesssim 7.8$ eV is firmly excluded by the observations, effectively closing this window of axion mass (for $\zeta = 1$).

Having now established that the existence of the "simplest" axion ($E/N = \frac{8}{3}, \zeta = 1$) is excluded by the data, what additional information can be extracted from our data about axions arising in more complicated models ($\zeta < 1$)? The model dependence will turn out to be slight, since any bound to the axion mass based on Eq. (19) will

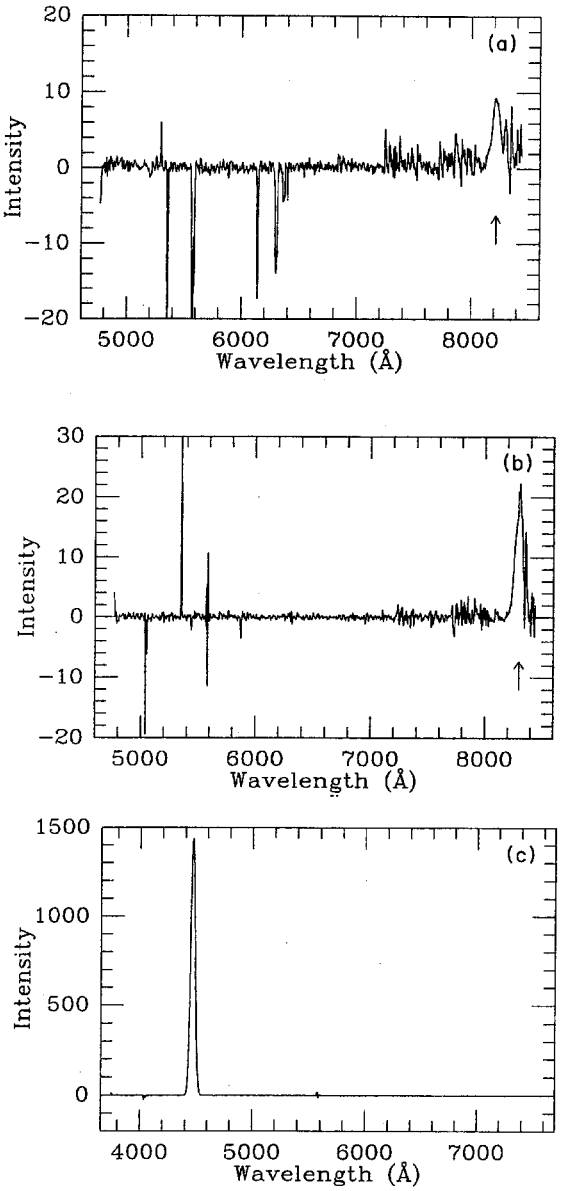

FIG. 8. Three on-off spectra with an axion decay line obeying Eq. (19) (with $\zeta = 1$) artificially introduced into each spectrum. Intensity is in units of 10^{-18} erg cm^{-2} arc sec^{-2} Å^{-1} sec^{-1}. (a) A2256, night 1 with a 3.2-eV axion decay line added (indicated by arrow). This spectrum constitutes the low mass limit in this axion search [compare with Fig. 7(c)]. (b) A2218, night 1 with a 3.5-eV line added (indicated by arrow) [compare with Fig. 7(b)]. (c) A2218, night 2 with a 6.5-eV line added (compare with Fig. 7(e) and Fig. 5).

vary as $m_a \propto \zeta^{-2/7}$. Since no cluster line is in evidence in Fig. 7, we cannot simply read off the value of ζ by comparing the line intensity with that predicted. The best alternative to this is to determine the limit which the data places on any line emission in the cluster and, via Eq. (19), use these limits to determine the minimum value of ζ that would produce a line at or below this intensity level. This problem will be attacked in two manners. First I will discuss a cross-correlation technique where the spectra of Fig. 7 are correlated with each other and noiseless "template" spectra in search of a correlation peak which would indicate cluster line emission. The cross-correlation technique is well suited to detecting a cluster emission line but is too time consuming to establish absolute line-flux limits throughout the spectrum. The second method I will discuss is simply to run a moving window, with a width equivalent to an axion decay line, across each spectrum and calculate the mean flux in each window. The "two-σ" upper bound on this flux is then a firm bound on any intergalactic line flux in the cluster and can be used to constrain ζ.

The use of Fourier cross-correlation techniques to pull signals out of the noise is often used in many spectroscopic applications [41,42]. In searching for intracluster line emission the application of this technique is simple and straightforward. While the wavelength of the would-be line is unknown, a line intrinsic to the cluster will appear at different wavelengths in different clusters, $\lambda_i = \lambda_a(1+z_i)$. Upon taking the logarithm of this equation we find $\ln\lambda_i = \ln\lambda_a + \ln(1+z_i)$. If the spectral dimension of the spectrum is converted to the logarithm of λ, lines in different clusters will be offset by a constant, *known* amount no matter what the intrinsic wavelength of the line. Since this is the case, an intracluster line will lead to a positive peak in the cross-correlation function of the on-off spectra for any two clusters,

$$\xi(l) = \frac{\int I_1(x) I_2(x+l)\,dx}{\left[\int I_1^2 dx \int I_2^2 dx\right]^{1/2}} = \frac{\int I_1(k)^* I_2(k)\exp(-ikl)\,dk}{\left[\int |I_1(k)|^2 dk \int |I_2(k)|^2 dk\right]^{1/2}}, \tag{20}$$

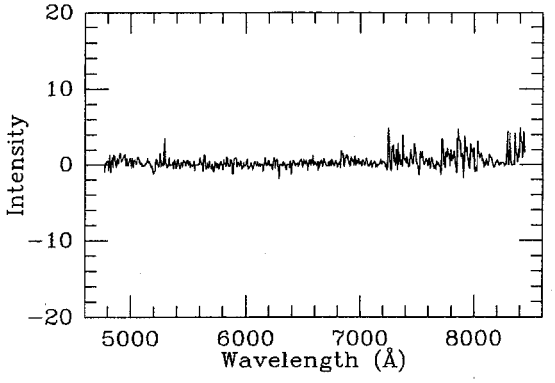

FIG. 9. The on-off spectrum of A2256, night 1 with obvious cosmic-ray hits and poorly subtracted night sky lines removed [compare with Fig. 7(c)].

at a lag $l = \ln[(1+z_2)/(1+z_1)]$, where the variable is $x = \ln\lambda$. Moreover, the height and width of the peak in $\xi(l)$ are directly related to the intensity and width of the intracluster emission line. A statistically significant peak at the correct lag and of the proper width would provide strong evidence for an intracluster line. If such a peak was found in $\xi(l)$, the spectra could then be carefully searched in order to determine λ_i, the wavelength of the line, and then m_a.

To assess the statistical significance of a peak, one must know the distribution of false peaks due to noise. In each of our on-off spectra all of the prominent features which are obviously associated with cosmic-ray hits or poor night sky subtraction have been removed. In Fig. 9 I show the on-off spectrum of A2256 with major cosmic-ray hits and night sky lines removed [compare this with Fig. 7(c)]. The central limit theorem then ensures that the remaining noise peaks have a Gaussian distribution. Hence, the probability of a positive noise peak of height

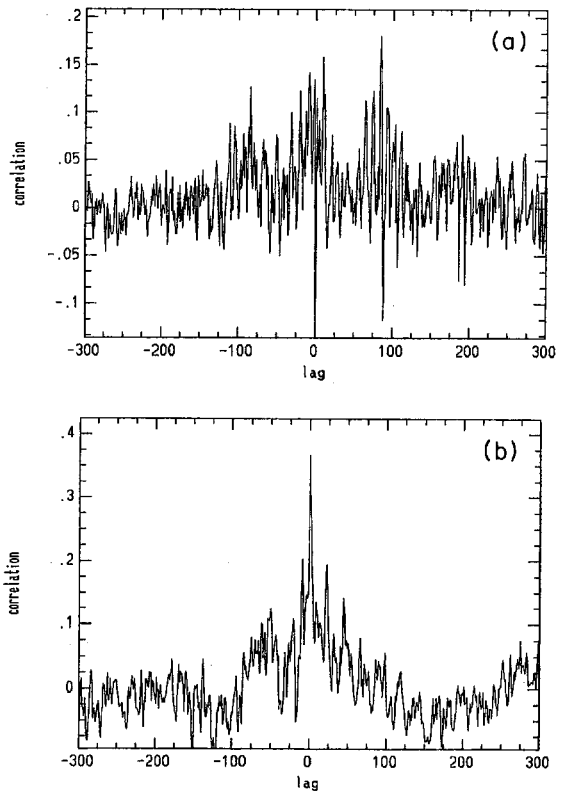

FIG. 10. The cross-correlation function $\xi(l)$ for two sets of clusters. The lag is in pixels and the correlation $= h \leq 1$. (a) The night 1 data of A2218 and A2256 cross correlated. A correlation peak arising from intracluster line emission would be centered at a lag of 138 with a width of $\sim$30 pixels [compare with Fig. 11(a)]. (b) The night 2 data of A1413 and A2218 cross correlated. A correlation peak from intracluster line emission would reside at a lag of 27 pixels. The narrow peak at lag $= 0$ is due to residual night sky lines.

greater than h is

$$P(>h)=\int_h^\infty \frac{\exp(-h^2/4\sigma_\xi^2)dh}{\sqrt{\pi}\sigma_\xi}=\text{erfc}\left[\frac{h}{2\sigma_\xi}\right], \quad (21)$$

where σ_ξ is the rms of the antisymmetric part of $\xi(l)$. In computing σ_ξ one must eliminate the possible contribution of real signals. This is done by calculating the rms value of the asymmetric part, $\xi_{\text{asym}}(l)=[\xi(l_0+l)-\xi(l_0-l)]/2$, where l_0 is the lag expected for a real signal, and assuming that the rms value of the symmetric part is the same. Any real signal does not contribute because its asymmetric part vanishes. A more detailed discussion of this technique and the underlying theory is given in Ref. [41].

In Figs. 10(a) and (b) I show two cross-correlation functions between on-off spectra of clusters. Figure 10(a) is the night 1 spectra of A2218 and A2256 cross correlated; Fig. 10(b) is the night 2 spectra of A1413 and A2218 cross correlated. For comparison, in Fig. 11 I include two correlation functions with artificial axion lines introduced. In Fig. 11(a) I correlate the night 1 on-off spectra of A2256 and A2218 with a 3.5-eV axion decay line added to each. In Fig. 11(b) I include a 6.0-eV axion decay line with $\zeta=0.07$ ($E/N=2$) in the night 2 on-off spectra of A2218 and A1413. In both cases the correlation peak clearly stands out.

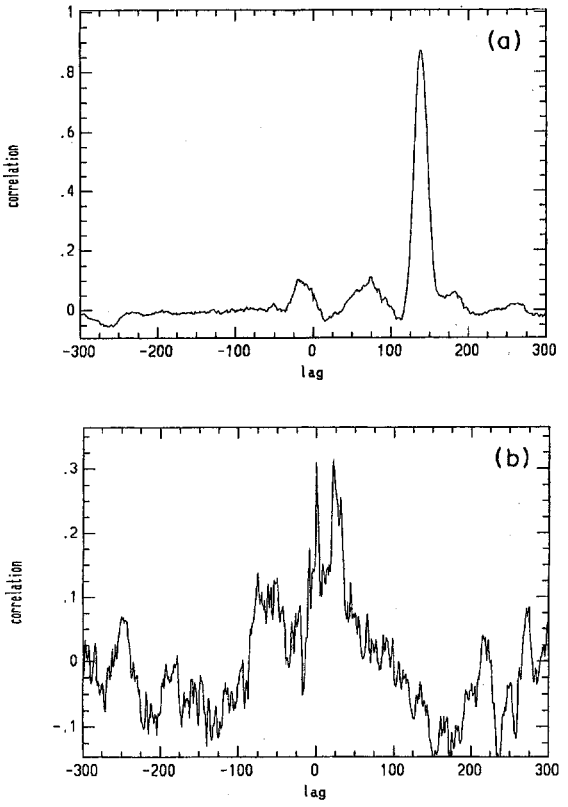

FIG. 11. $\xi(l)$ for two sets of clusters, each set with an axion line artificially introduced into the spectra. (a) A2218 and A2256, each with a 3.5-eV, $\zeta=1$ axion line in it [see Fig. 8(b)]. The lag is in pixels and correlation$=h$. The correlation peak is centered at lag$=138$ pixels and is highly significant ($h/2\sigma_\xi=11.9$) [compare with Fig. 10(a)]. (b) $\xi(l)$ for the night 2 data of A2218 and A1413 with a 6.0-eV, $\zeta=0.07$ axion line added to each. The peak is centered at lag$=27$ pixels and is highly significant, $\mathcal{P}(>h)\simeq 1.8\times10^{-5}$ ($h/2\sigma_\xi=3.04$) [compare with Fig. 10(b)].

TABLE III. Summary of limits to the flux and the parameter ζ from the cross-correlation technique.

m_a	Flux	ζ	Cluster
3.5	1.35×10^{-18}	0.16	A2256
4.0	8.0×10^{-19}	0.078	A2218
4.5	4.6×10^{-19}	0.039	A2218
5.0	6.6×10^{-19}	0.032	A2218
6.0	5.9×10^{-19}	0.016	A2218
7.5	1.3×10^{-18}	0.011	A2218

The cross correlation is carried out using the rvxcor computer task in IRAF. This task takes the two spectra to be correlated and returns $\xi(l)$ (as in Figs. 10 and 11), the lag of the correlation peak in pixels (which can then be converted into Å), the normalized peak height $h(0\le h\le 1)$, and the value of σ_ξ. Using data with artificial axion lines introduced, it is simple to determine the correct lag of the peak (in pixels) for the correlation of cluster with cluster. Having determined the location of the presumed peak, a Gaussian is fit to this region of $\xi(l)$ for the unaltered spectra to determine both h and σ_ξ. These two quantities can then be used to determine the statistical significance of any peak present. The criteria that a "real" correlation peak must satisfy are that it must be within 1σ of the correct lag and it must have less than a 5% chance of being a noise peak [$\mathcal{P}(>h)\le 0.05$]. This corresponds to a 2σ or greater probability that the peak is due to a real correlation and is not a spurious noise peak. No peak meeting these criteria is present in

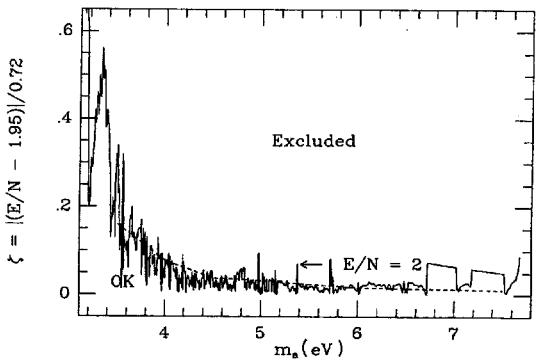

FIG. 12. The values of ζ required to hide an axion line in the observed clusters of galaxies. The dashed line is from cross correlating spectra with noiseless templates (see Table III). The solid line arises from the flux limits of Figs. 13(a)–(e) (see text for details).

the correlation functions of Fig. 10. As an example, when a fit is done to the correlation peak nearest the correct lag for the night 1 data of A2218 and A2256, the fitted peak is at a lag 15% too small and has a height in the noise-peak distribution where there is a 39% probability of having a peak of this height or larger. This peak is clearly not from an intracluster emission line.

To set flux limits using the cross-correlation technique, I have modified the procedure somewhat. Instead of correlating the cluster spectra with one another, I correlate one of the cluster spectra with an axion decay line inserted against a noiseless "template" spectrum containing the same mass line [the template is simply the line described by Eq. (19b) with nothing else added]. The strength of the line is then reduced until the height of the cross-correlation peak is such that there is only a 5% chance that the peak is due to the Gaussian noise. The intensity at which this happens then constitutes the 2σ

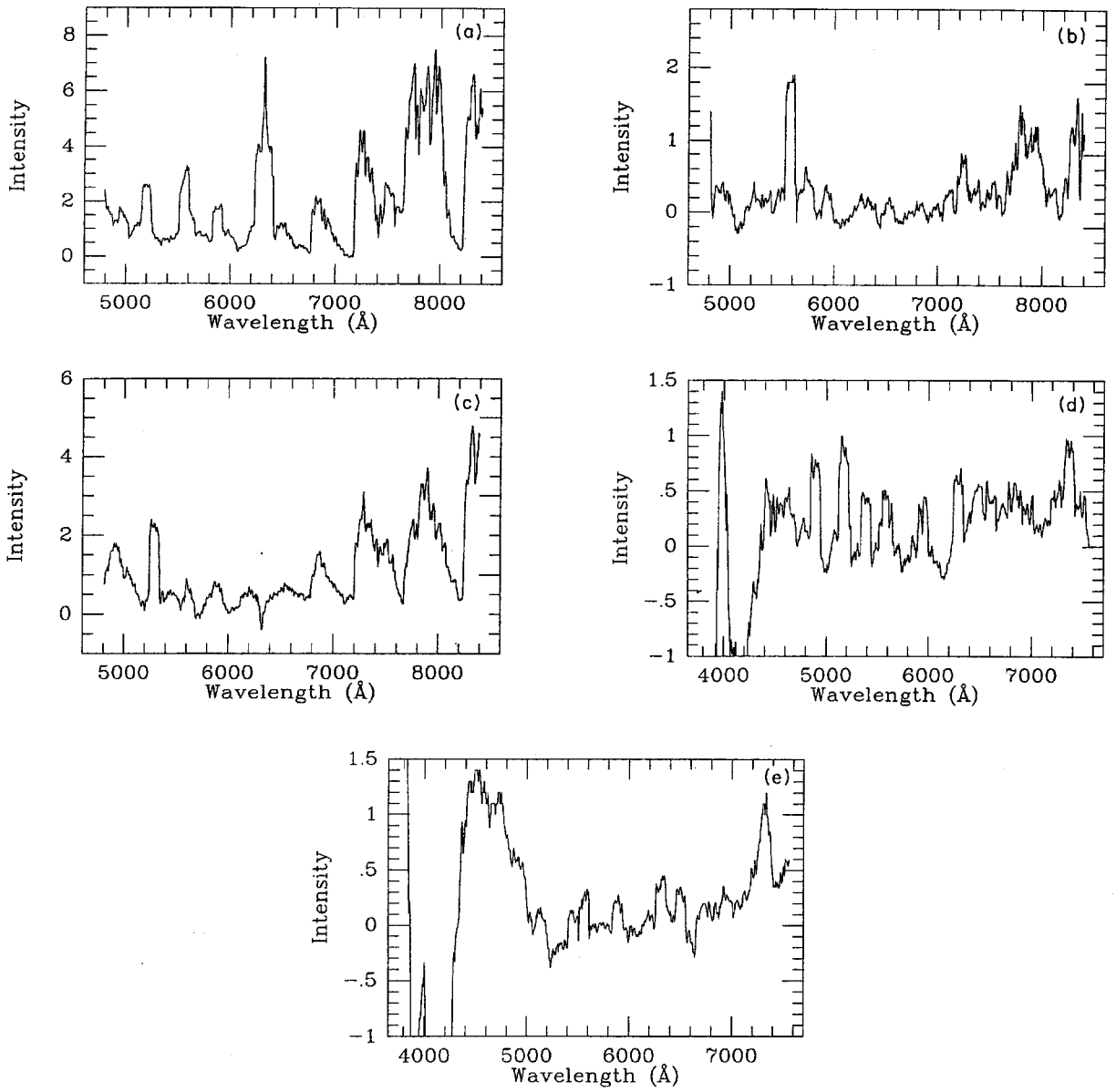

FIG. 13. 2σ limits to any line flux arising in the five observed clusters of galaxies (see text for details). (a) A1413, night 1; (b) A2218, night 1; (c) A2256 night 1; (d) A1413, night 2; (e) A2218, night 2. The large regions with negative flux in the night 2 data are due to problems with the dome flat in the blue (see text for details). Intensity is in units of 10^{-18} erg cm^{-2} arc sec^{-2} Å^{-1} sec^{-1}.

limit to any line flux at that wavelength. These limits on the flux may then be turned into limits on the model parameter ζ. This procedure has been carried out for a number of axion masses using the data; the most restrictive limits are summarized in Table III and Fig. 12 by the dashed line (these results were also presented in Ref. [15]).

The cross-correlation method discussed above produces quite stringent limits on the flux of intracluster light and hence on the parameter ζ. An examination of Fig. 12 reveals that axions more massive than 4 eV seem to be excluded by the data, even for $E/N=2$ ($\zeta=0.07$). The disadvantage of this technique is that finding absolute limits for every value of m_a is time consuming; one must construct template spectra at the central wavelength of the 796 pixels of each spectrum and cross correlate them with the spectrum. As an alternative to this, I now investigate another way of getting limits to any line flux in the on-off spectra.

The spectra of Figs. 7(a)–(e) represent useful limits to the presence of any line flux in the three clusters of galaxies observed. One method of quantifying the amount of flux in each of the spectra is to sequentially examine a series of small "windows" in the spectra, each with a width roughly equivalent to that of an intracluster emission line. The FWHM of an axion line intrinsic to a cluster of galaxies is 210 Å $\sigma_3(\mathrm{eV}/m_a)(1+z)$. For axions in the multi-eV window this line width will vary between about 40 and 90 Å. This suggests that by examining the flux in a small window of the spectra of width 90 Å (20 pixels) a limit to the flux of an axion line in this window can be obtained. In each window, the mean intensity per pixel $\bar{I}$ and the standard deviation from the mean per pixel σ_I can be calculated. The total integrated flux in the window is then given by $F_W=(4.6\ \text{Å/pixel})\times 20\ \text{pixels}\times\bar{I}$ with a standard deviation given by $\sigma_W=(4.6\ \text{Å/pixel})\times\sqrt{20\ \text{pixels}}\times\sigma_I$. σ_W is used to determine the distribution of noise in the spectrum. We can now use F_W and σ_W to set quantitative limits to any line flux in the window by comparing F_W with the integrated flux that a cluster emission line would produce in the window. The probability that a cluster emission line with a flux F_a would produce a detected flux of less than F_W in the data is

$$\mathcal{P}(F_a,F_W)=\frac{1}{\sqrt{2\pi}\sigma_W}\int_{-\infty}^{F_W-F_a}\exp\left[\frac{-h^2}{2\sigma_W^2}\right]dh\ ,$$

where the distribution of noise peaks is taken to be Gaussian. (This expression derives from requiring that the noise, when added to the signal F_a results in a detected flux of F_W or less.) In order to set 95% confidence limits to the presence of any line flux (similar to those derived via cross correlation), I require that only 5% of the time is a downward fluctuation of the noise sufficient to suppress a signal to a flux less than that observed, F_W [i.e., $\mathcal{P}(F_a,F_W)=0.05$]. This occurs when $F_W-F_a=-1.65\sigma_W$. Thus any cluster emission line with a flux $1.65\sigma_W$ greater than that observed in the window can be excluded at the 95% confidence level. Now that we can calculate a limit to any flux in a 20-pixel window, we can move such a window throughout an entire spectrum, one pixel at a time, and derive limits to the amount of line emission in each of the subtracted spectra of Figs. 7(a)–(e). In Figs. 13(a)–(e) I present the 95% confidence limits to any line flux in the observed clusters by this technique. In Figs. 13(d) and (e), the large downward (and negative) fluctuations in the blue are due to the problems with the dome flats alluded to earlier. Note that the flux levels in Fig. 13 are comparable to those obtained via the cross-correlation analysis.

The flux limits displayed in Fig. 13 provide a means of determining firm limits to ζ, the axion model dependence parameter. By comparing each of the five on-off spectra at points corresponding to a single axion mass and by choosing the lowest value of the flux at this point, the maximum value of I_a consistent with the observations can be identified. Equation (19) can then be used to determine the maximum value of ζ which produces an axion decay line with an intensity equal to the observational limit. The results of this exercise are displayed in Fig. 12. The two bumps in ζ near $m_a=7$ eV arise from the overlap of the regions of negative flux in Figs. 13(d) and (e). Since the data is unreliable here, I have simply taken the flux limit to be the level of the night sky continuum, $I_{\mathrm{NS}}=10^{-17}$ erg cm^{-2} arc sec^{-2} Å^{-1} sec^{-1}. The values of ζ are still less than for the $E/N=2$ case. It is clear from this figure that the maximum axion masses allowed for $E/N=2$ are $m_a\lesssim 4$ eV, far below the equivalent bounds from RG-HB stellar evolution. Finally, it is worth remembering that I have chosen the mass fraction of axions in clusters very conservatively ($=\Omega_a$). The mass fraction could be up to a factor of 10 larger. If this is the case, the limits to ζ would improve by a factor of about 3 since, for a given m_a, $\zeta\propto\sqrt{I_a}$.

As a final topic, I will discuss the possibility that the axions are not distributed like the luminous matter in the cluster. All of the limits considered so far assume that the axions have a spatial distribution similar to the galaxies and x-ray gas in the cluster, $\Sigma_a\propto 1/R^2$ or $1/R$ for $R>a$, where a is determined by the luminous material. While this seems, by far, the most reasonable assumption, it may not be the case. Axions could, for example, have a similar spatial distribution but with $a_{\mathrm{axion}}\gg a_{\mathrm{galaxies}}$. This could occur if, for example, the majority of the mass in the cluster, M, consisted of cold dark matter (CDM). West and Richstone [43] have shown that, for $M_{\mathrm{CDM}}\gg M_{\mathrm{galaxies}}$, dynamical friction may lead to a strong segregation of the galaxies to the central regions of the cluster (this could also affect the x-ray gas if it is "blown out" of the galaxies after cluster formation). Since the axions would be distributed more diffusely than the baryons (in one model of Ref. [43], $a_{\mathrm{axions}}\sim a_{\mathrm{CDM}}\sim(5-10)a_{\mathrm{galaxies}}$), the predicted axion signal would be smaller ($I_a\propto 1/a_{\mathrm{axion}}$), and the subtraction would almost totally remove the line, significantly altering the limits quoted.

This concern can be addressed by subtracting the data of one cluster from that of another cluster. Since any line due to the same physical process in the two clusters will

be redshifted to different wavelengths, the line will not be removed by the subtraction. In fact, this procedure produces a unique signature for a cluster emission line: a pair of lines, one positive and one negative, corresponding to a single rest wavelength. In Figs. 14(a) and (b) I show two such spectra: (a) the inner aperture of A2256 minus the outer aperture of A1413, and (b) the inner aperture of A2218 minus the outer aperture of A2256. Both are from the first night's data. These two sets of spectra were chosen because they were taken close together in time, if not in space. There are two important features to notice in the on-off spectra of Fig. 14. First, the night sky subtraction is significantly poorer than the same cluster subtractions due to the large spatial separation of the apertures (a factor of ~ 4 worse, as quantified by the moving window technique). Note also, that the base-line value of the subtractions is once again close to 0 [although not as convincingly as in Figs. 7(a)–7(e)]. Second, there is absolutely no indication of the existence of any intracluster line emission in either of the spectra. Since the axion core radius is being treated as an unknown here, no real predictions of I_a can be made for the clusters. Hence, no statement concerning limits to ζ can be made based upon the data if the axions do not track the light.

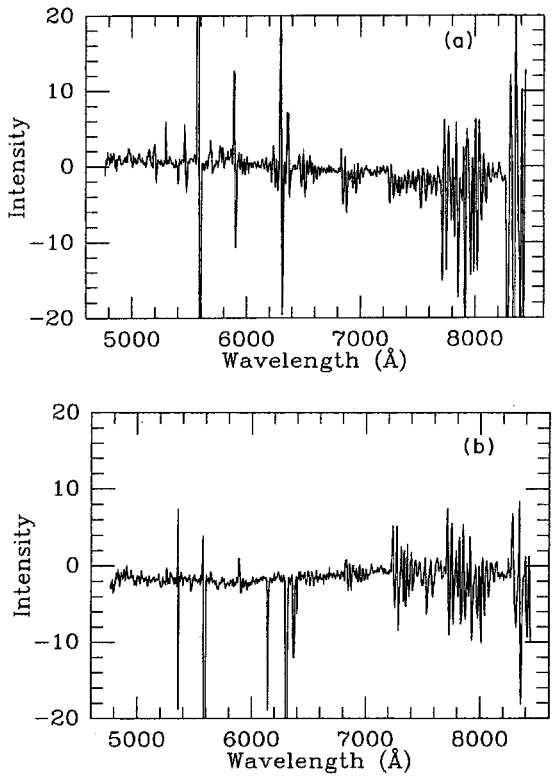

FIG. 14. (a) A night 1 spectrum from A2256 minus that of A1413. (b) A night 1 spectrum of A2218 minus that of A2256. Intensity is in units of 10^{-18} erg cm^{-2} arc sec^{-2} Å^{-1} sec^{-1}.

V. CONCLUDING REMARKS

Astrophysics and cosmology have much to say about the axion. In this paper I have considered the relic decays of axions to photons in a number of astrophysical settings. By considering the effects of multi-eV axions diffusely spread throughout the cosmos and tightly clustered in the galactic halo, an upper limit to the axion mass of ~ 8 eV is obtained, even with the most pessimistic model dependence ($E/N=2$). In concert with the axion mass bound from SN 1987A ($m_a \gtrsim 3$ eV), these considerations lead to a well-defined window of allowed axion mass, $3 \lesssim m_a \lesssim 8$ eV.

This window has been unsuccessfully searched by looking for an emission line from axion decay in the intergalactic light of three clusters of galaxies. No signal matching that expected from axion decay is seen in the clusters, ruling out the existence of the axion (in the simplest models, $E/N=\frac{8}{3}$) in the mass range 3.2–7.8 eV. This implies, that if the axion exists, its mass lies in the range 10^{-3}–10^{-6} eV and that it likely comprises the majority of the dark matter known to exist in the Universe. Limits to the flux of any intracluster line emission were obtained by two techniques: by cross correlating spectra and by measuring the mean flux in a moving window throughout the spectra. It should be stressed that these line-flux limits are very dependent upon knowing the spatial distribution of the emitting source, axions or otherwise. It is highly likely that the intergalactic matter should track the luminous matter (galaxies and x-ray gas), and this assumption has been used throughout. Under this assumption, the flux limits lead to interesting limits upon the axion model dependence parameter ζ (or E/N). By insisting that the flux of any axion line be less than the observed flux in the cluster, it is found that even for $\zeta=0.07$ ($E/N=2$) axions with masses greater than 4 eV are excluded by the data. Finally, the question of whether the galaxies and gas in the cluster trace the mass has been addressed by subtracting one cluster's spectrum from another's spectrum; no evidence for line emission is seen. The remaining astrophysical uncertainty of note is the mass fraction of axions in the clusters. This fraction has been treated very conservatively and could be up to a factor of 10 larger than has been assumed. If the axion mass fraction in clusters was $\sim 10\Omega_a$ instead of Ω_a, axion masses significantly below 3 eV could be probed by this method [an axion of $m_a=2.3$ eV would produce a decay line with the same intensity as the 3.2-eV line predicted by Eq. (19b)].

A last concern I will address is the possibility that the window is not quite closed. I have used throughout the lower bound to the window of 3 eV. I have also stated that the data only extends to axion masses of 3.2 eV. (The data actually extends to $m_a=3.1$ eV, but the noise is too large to convincingly rule out an axion this massive, although there is no evidence for one.) Could the axion lie in this last small bit of parameter space? This concern could be exacerbated if the uncertainties in the SN 1987A analysis all tended to push that limit in the direction of lower axion mass. The answer to the above question is "yes, it might," although the remaining pa-

rameter space is quite small. Unfortunately, due to the large amount of noise in the red portion of the spectrum this question is unlikely to be answerable by ground-based observations. Another method would be needed to probe this range of axion mass (e.g., the proposed experiment of Ref. [40]), or the Hubble Space Telescope (HST) might answer the question once it is fitted with instruments which see farther into the red. High above the Earth's atmosphere HST would be free of the variable night sky and could thus obtain much better subtractions, allowing the region $m_a < 3.2$ eV to be probed. As an example, if HST's subtractions red-ward of 8400 Å were comparable to the best subtractions obtained in the blue portion of this investigation, line intensities of $\sim 10^{-18}$ erg cm^{-2} arc sec^{-2} Å^{-1} sec^{-1} should be detectable. (This value is typical of the limits obtained by the cross-correlation analysis in the quiet portions of the spectrum. See Table III.) One could then probe down to axion masses of ~ 2.5 eV ($\zeta = 1$), corresponding to $\lambda = 10\,600$ Å in A2256.

As a final comment upon this work I mention that, while everything done here has been specific to the axion, all of the results can be carried over to any relic particle which decays to optical photons. Equation (19) can be generalized to another relic X by multiplying it by $(n_\gamma/2)(\Omega_X/\Omega_a)(\tau_a/\tau_X)$, where $n_\gamma = 1$ or 2 is the number of photons produced in each X decay. The limits which this data places upon the lifetime of a relic neutrino that decays into a lighter neutrino and a photon will be considered elsewhere [15].

ACKNOWLEDGMENTS

It is a pleasure to thank my advisor, Michael S. Turner, and Matthew Bershady for a fruitful collaboration and much assistance in this project. Thanks are also due B. Yanny, M. Fitzpatrick, A. Dressler, and the staff at KPNO for assistance. The finishing touches were placed upon this work at the Aspen Center for Physics. This research was supported by NASA (Grant No. NGW-1340 at Fermilab and through the GSRP), and by the DOE at Chicago and Fermilab. KPNO of the National Optical Astronomy Observatories is operated by AURA, Inc., under contract with the NSF.

[1] M. S. Turner, Phys. Rep. **197**, 67 (1990).
[2] G. G. Raffelt, Phys. Rep. **198**, 1 (1991).
[3] R. D. Peccei and H. R. Quinn, Phys. Rev. Lett. **38**, 1440 (1977).
[4] G. 't Hooft, in *Recent Developments in Gauge Theories*, Proceedings of the Cargese Summer Institute, Cargese, France, 1979, edited by G. 't Hooft *et al.*, NATO Advanced Study Institutes, Series B: Physics, Vol. 59 (Plenum, New York, 1979), p. 135.
[5] H.-Y. Cheng, Phys. Rep. **158**, 1 (1988).
[6] F. Wilczek, Phys. Rev. Lett. **40**, 279 (1978); S. Weinberg, *ibid.* **48**, 223 (1978).
[7] M. Dine, W. Fischler, and M. Srednicki, Phys. Lett. **104B**, 199 (1981); A. Zhitnitsky, Yad. Fiz. **31**, 497 (1980) [Sov. J. Nucl. Phys. **31**, 260 (1980)].
[8] J.-E. Kim, Phys. Rev. Lett. **43**, 103 (1979); M. Shifman, A. Vainshtein, and V. Zakharov, Nucl. Phys. **B166**, 493 (1980).
[9] D. Kaplan, Nucl. Phys. **B260**, 215 (1985).
[10] E. W. Kolb and M. S. Turner, *The Early Universe* (Addison-Wesley, Redwood City, CA, 1990), pp. 422–36.
[11] M. S. Turner, Phys. Rev. D **33**, 889 (1986).
[12] M. S. Turner, Phys. Rev. Lett. **59**, 2489 (1987).
[13] T. W. Kephart and T. J. Weiler, Phys. Rev. Lett. **58**, 171 (1987).
[14] A. L. Broadfoot and K. R. Kendall, J. Geophys. Res. **73**, 426 (1968); P. Massey, C. Gronwall, and C. A. Pilachowski, Publ. Astron. Soc. Pac. **102**, 1046 (1990); S. Louistisserand *et al.*, Astron. Astrophys. Suppl. Ser. **68**, 539 (1987).
[15] M. A. Bershady, M. T. Ressell, and M. S. Turner, Phys. Rev. Lett. **66**, 1398 (1991); and (work in progress).
[16] A. Burrows, M. T. Ressell, and M. S. Turner, Phys. Rev. D **42**, 3297 (1990).
[17] G. G. Raffelt and D. S. P. Dearborn, Phys. Rev. D **36**, 2211 (1987).
[18] W. C. Haxton and K. Y. Lee, Phys. Rev. Lett. **66**, 2557 (1991).
[19] J. Engel, D. Seckel, and A. C. Hayes, Phys. Rev. Lett. **65**, 960 (1990).
[20] D. A. Dicus, E. W. Kolb, V. L. Teplitz, and R. V. Wagoner, Phys. Rev. D **22**, 839 (1980). Note that these authors' upper bound to the axion mass is too low due to the failure to include plasma screening effects; see Ref. [17].
[21] M. S. Turner, Phys. Rev. Lett. **60**, 1797 (1988).
[22] M. T. Ressell and M. S. Turner, Comments Astrophys. **14**, 323 (1990).
[23] R. Kimble, S. Bowyer, and P. Jakobsen, Phys. Rev. Lett. **46**, 80 (1981).
[24] J. N. Bahcall, Annu. Rev. Astron. Astrophys. **24**, 577 (1986); G. Gilmore, I. R. King, and P. C. van der Kruit, *The Milky Way as a Galaxy* (University Science Books, Mill Valley, CA, 1990).
[25] S. Tremaine and J. E. Gunn, Phys. Rev. Lett. **42**, 407 (1979).
[26] J. Madsen, Phys. Rev. Lett. **64**, 2744 (1990).
[27] Kolb and Turner, *The Early Universe* [10], pp. 64–5.
[28] Kolb and Turner, *The Early Universe* [10], pp. 87–113.
[29] J. Binney and S. Tremaine, *Galactic Dynamics* (Princeton University Press, Princeton, NJ, 1987), Chaps. 1, 2, and 4.
[30] D. Lynden-Bell, Mon. Not. R. Astron. Soc. **136**, 101 (1967).
[31] C. L. Sarazin, Rev. Mod. Phys. **58**, 1 (1986); C. L. Sarazin, *X-ray Emissions from Clusters of Galaxies* (Cambridge University Press, Cambridge, England, 1988).
[32] P. J. Quinn, J. K. Salmon, and W. H. Zurek, Nature (London) **322**, 329 (1986); W. H. Zurek, P. J. Quinn, and J. K. Salmon, Astrophys. J. **330**, 519 (1988); C. S. Frenk, S.D.M. White, G. Efstathiou, and M. Davis, Nature (London) **317**, 595 (1985).
[33] M. J. West, A. Dekel, and A. Oemler, Jr., Astrophys. J. **316**, 1 (1987).

[34] C. L. Sarazin, Rev. Mod. Phys. **58**, 1 (1986); A. Dressler, Astrophys. J. **223**, 765 (1978); **226**, 55 (1978); C. Jones *et al.*, Astrophys. J. Lett. **234**, L21 (1979); J. M. Uson and S. B. Boughn, Report No. NRAO-90/121, 1990 (unpublished); T. C. Beers and J. L. Tonry, Astrophys. J. **300**, 557 (1986).

[35] Sarazin [34]; S. M. Lea and J. P. Henry, Astrophys. J. **332**, 81 (1988); P. E. Boynton *et al.*, *ibid.* **257**, 473 (1983); L. A. Thompson, *ibid.* **306**, 384 (1986); Dressler [34]; Uson and Boughn [34]; Beers and Tonry [34].

[36] Sarazin [34]; D. G. Fabricant, S. M. Kent, and M. J. Kurtz, Astrophys. J. **336**, 77 (1989); A. Dressler, Astrophys. J. Suppl. **42**, 565 (1980); and [34]; Jones *et al.* [34]; C. Jones and W. Forman, Astrophys. J. **276**, 38 (1984); Beers and Tonry [34].

[37] R. C. Henry and P. D. Feldman, Phys. Rev. Lett. **47**, 618 (1981); J. B. Holberg and H. B. Barber, Astrophys. J. **292**, 16 (1985).

[38] H. L. Shipman and R. Cowsik, Astrophys. J. **247**, L111 (1981); R. B. Partridge, in *IAU Symposium 139, Galactic and Extragalactic Background Radiation,* edited by S. Bowyer and C. Leinert (Kluwer, Doredrecht, 1990).

[39] P. Massey and C. Gronwall, Astrophys. J. **358**, 344 (1990); P. Massey *et al.*, *ibid.* **328**, 315 (1988).

[40] K. van Bibber, P. M. McIntyre, D. E. Morris, and G. G. Raffelt, Phys. Rev. D **39**, 2089 (1989).

[41] J. Tonry and M. Davis, Astron. J. **84**, 1511 (1979).

[42] J. M. Brault and O. R. White, Astron. Astrophys. **13**, 169 (1971); S. J. Simkin, *ibid.* **31**, 129 (1974).

[43] M. J. West and D. O. Richstone, Astrophys. J. **335**, 532 (1988).